WAVE PROPAGATION ALONG A SHIELDED COAXIAL CABLE WITHIN A CIRCULAR WAVEGUIDE

by

JEN - HWANG LEE

B.S.E.E., National Chiao-Tung University, Taiwan, 1972

A MASTER'S THESIS

submitted in partial fulfillment of the

requirements for the degree

MASTER OF SCIENCE

Department of Electrical Engineering

KANSAS STATE UNIVERSITY
Manhattan, Kansas
1976

Approved by:

Kendall F. Casey
Major Professor

TABLE OF CONTENTS

CHAPTER 1

INTRODUCTION

A great deal of work on wave propagation within a tunnel structure has been carried out in the past few years. The purpose of this work is to search for an understanding of the wave behavior inside a real tunnel through study of some idealized structures, and then to find an optimum condition for long distance communication within a tunnel. Firstly, the wave propagation problem along an infinitely long straight wire located inside a rectangular waveguide with perfectly conducting boundaries was investigated by Mahmoud[1] in 1973. He deduced a modal equation for the propagation constants along the wire. This conducting wire is obviously important if the frequency is sufficiently low that the modes for the empty guide are cut off, because the presence of the wire allows a TEM mode to exist inside the guide. About the same time, Wait[2] considered the tunnel as a circular cylinder in a lossy dielectric medium. A relatively thin metal conductor was located within this uniform tunnel. Then he calculated the complex propagation constants of the dominant modes of the structure. It is evident that the transmission of electromagnetic waves in

a real tunnel structure is very complicated, but it is worthwhile to investigate these idealized models of the situation.

Then Wait[3] carried out an analysis of the axial propagation characteristics of a two-wire transmission line in a circular tunnel bounded by lossy dielectric media. The two transmission-line modes corresponding to wire currents which are either in phase or 180° out of phase received a great deal of attention. Wait discovered that the attenuations of the two transmission-line modes are not equal and that one of them is strongly dependent on the location of the conductor, while the other is relatively insensitive to the conductor location. The excitation of the transmission-line modes in a circular tunnel was examined by Hill[4] in 1974. He found that the mode with higher attenuation rate is much easier to excite by an antenna placed in the tunnel than the mode with lower attenuation.

Wait[5] considered wave propagation along a braided coaxial cable in a circular tunnel. He developed an approximate impedance boundary condition at the surface of the cable which can be used in the formalisms which had been developed for axial conductors in tunnels.

In this paper we shall use a recently developed model

of the coaxial cable[6] in the analysis of wave propagation inside a circular tunnel. The external impedance of the coaxial cable has been determined from this cable model. The propagation constants of the transmission-line modes can be determined through the solution of an appropriate boundary-value problem. In order for the solution to be valid, the radius of the cable should be small compared with the distance to the tunnel wall. The fields in the vicinity of the cable are assumed to be uniform. In addition, for simplicity the propagations of the transmission-line modes are assumed to be unattenuated; i.e., the structure is taken to be lossless. We shall consider that a dipole source is located inside the tunnel, and the fields radiated by this source which are coupled to the coaxial cable will be investigated in this paper.

In the next chapter, we shall introduce two shielded coaxial cable models and describe the cable characteristics of these two models. In chapter 3, we shall formulate the problem and investigate the excitation and propagation problem inside the tunnel. Chapter 4 will present some numerical illustrations, and chapter 5 concludes the paper.

CHAPTER 2

THE SHIELDED COAXIAL CABLE

2.1 Physical structure of leaky braided-shield cable

The physical structure of the coaxial cable which we shall deal with in this paper consists of four parts. They are the center conductor, two dielectric layers, and the conducting shield. The center conductor with radius $\underline{r}$ is covered by a dielectric layer with free space permeability μ_o and permittivity ε_1; this dielectric layer is called the inner dielectric and it extends from ρ=r to $\rho = \rho_1$. The outer part of this cable is another dielectric layer called the outer jacket, extending from $\rho = \rho_1$ to ρ=b. This jacket has permittivity ε_2 and permeability μ_o. The conducting shield of this cable is located between the inner dielectric and the outer jacket. In the model we consider in this paper, the shield consists of two multifilar helical sets of conducting wires whose radii are much smaller than that of the cable. These two sets of shield wires surround the inner dielectric and make pitch angles $\pm\psi$ with the axis of the cable. The geometry is illustrated in Fig. 1. Here we assume that the optical

THIS BOOK CONTAINS NUMEROUS PAGES WITH DIAGRAMS THAT ARE CROOKED COMPARED TO THE REST OF THE INFORMATION ON THE PAGE.

THIS IS AS RECEIVED FROM CUSTOMER.

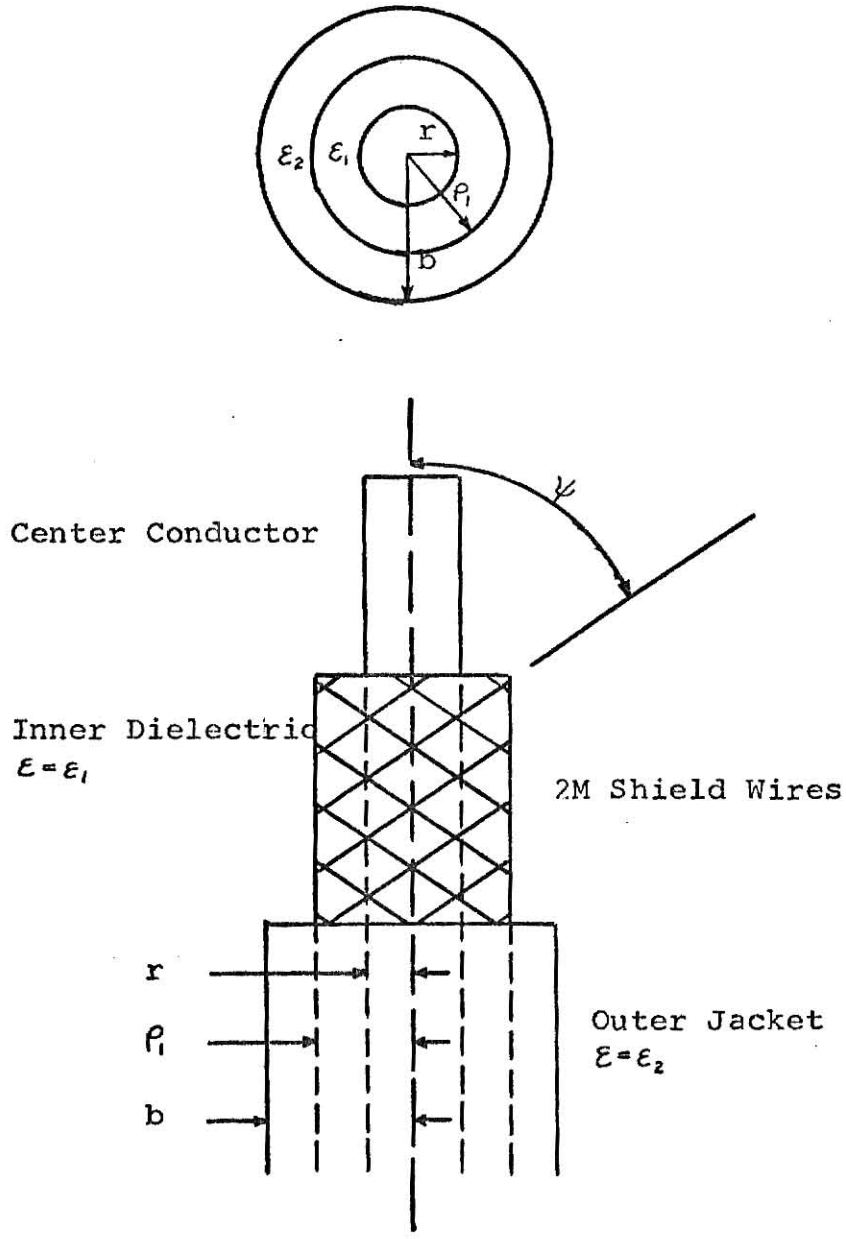

Fig. 1 Geometry of Multifilar Helix Shielded Cable

coverage of the shield is less than unity, which means that the shield does not completely cover the surface at $\rho = \rho_1$.

We shall briefly consider two models for these leaky coaxial cables in subsequent sections of this chapter, following a discussion of the transmission line parameters which are used to describe these cables in greater detail, and in which the cable characteristics will be formulated.

2.2 Transmission-line equations

The transmission-line equations we are going to solve in this paper may be written in the form:

$$\frac{dV}{dz} = -ZI - Z_s I_t^c \qquad (2.1)$$

$$\frac{dI}{dz} = -YV + j\omega\Gamma_s Q_t^c \qquad (2.2)$$

As usual, the time dependence $\exp(j\omega t)$ of all the field quantities is understood; and it will be suppressed throughout this paper. Here we use the cylindrical coordinate system; i.e., the (ρ,ϕ,z) system, and z is the axial coordinate.

In these equations, V denotes the voltage of the center conductor with respect to the shield, and I is the

current on the center conductor. Z and Y denote respectively the series impedance and shunt admittance per unit length of cable. Z_s is the transfer impedance per unit length of cable. Γ_s is the dimensionless capacitive coupling coefficient per unit length. I_t^c and Q_t^c are respectively the total current and the total charge per unit length on the cable.

From the continuity equation, we have

$$j\omega Q_t^c = - \frac{dI_t^c}{dz} \qquad (2.3)$$

The following relations will be found to be useful:

$$Z = Z_c + Z_s \qquad (2.4)$$

$$\frac{1}{Y} = \frac{1}{Y_c} + \frac{1}{Y_s} \qquad (2.5)$$

$$\text{and } \Gamma_s = \frac{Y}{Y_s} \qquad (2.6)$$

where Y_c, Y_s, Z_c, and Z_s are the transmission-line parameters of the coaxial cable. Y_c and Z_c are principally characteristic of the cable interior and the center conductor, while Y_s and Z_s are principally characteristic of the shield.

In section 4 of this chapter, we shall introduce the expression for the external impedance $\hat{Z}_{ex}$ in terms of these four transmission-line parameters which will be used in our analysis. The external impedance is the series impedance of the cable evaluated on its outer surface, and is defined by

$$\hat{Z}_{ex}(h) = \hat{E}_z(h)/\hat{I}_t^c(h) \qquad (2.7)$$

where $\hat{E}_z$ is the average Fourier-transformed axial electric field at the cable surface, and $\hat{I}_t^c$ is the Fourier transform of the total current I_t^c. $\underline{h}$ is the transform variable.

2.3 Wait's model for shield; $\hat{Z}_{ex}(h)$

The physical structure of the coaxial cable model which was considered by J.R.Wait[5] is illustrated in Fig. 2.

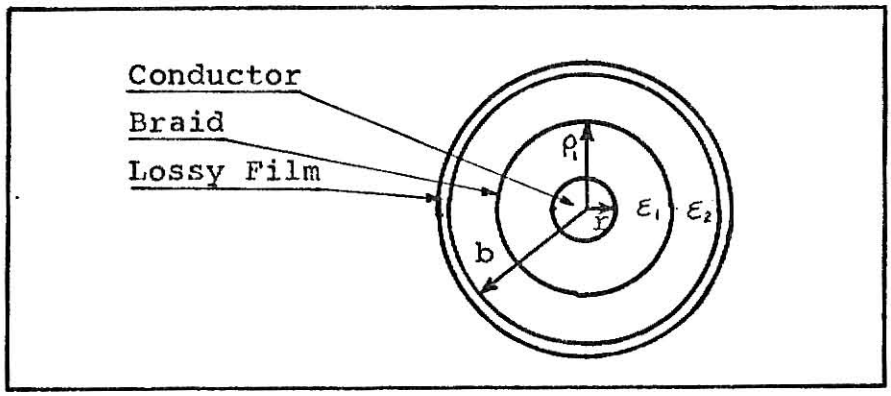

Fig. 2 Wait's Coaxial Cable Model

As in the model we introduced in section 2.1, the center conductor has radius $\underline{r}$, and is covered by a layer of perfect

insulation of radius ρ_1 with dielectric constant ε_1 and free-space permeability μ_o. The outer jacket with permittivity ε_2 and permeability μ_o surrounds this inner dielectric and the center conductor, and extends from $\rho = \rho_1$ to $\rho = b$.

The differences between this model and that which we consider in section 2.1 are that the braided shield at $\rho = \rho_1$ is assumed uniformly smoothed-out and that there is a thin outer layer of conductive material covering the cable. Furthermore, the uniform braided shield is assumed to be described by a transfer impedance Z_T, and the external lossy film has transfer impedance Z_L ohms per meter.

From this coaxial cable model, Wait developed an expression for the external impedance $\hat{Z}_{ex}(h)$. In the low frequency case, his expression is given by

$$\hat{Z}_{ex}(h) \simeq \frac{Z_L(Z_2 + Z_b)}{Z_L + Z_2 + Z_b} \qquad (2.8)$$

where $$Z_b = \frac{Z_T(Z_1 + Z_i)}{Z_T + Z_1 + Z_i} \qquad (2.9)$$

with $$Z_1 = -\frac{k_1^2 - h^2}{2\pi j \omega \varepsilon_1} \ln\left(\frac{\rho_1}{r}\right) \qquad k_1 = \omega\sqrt{\mu_o \varepsilon_1} \qquad (2.10)$$

and $$Z_2 = -\frac{k_2^2 - h^2}{2\pi j \omega \varepsilon_2} \ln\left(\frac{b}{\rho_1}\right) \qquad k_2 = \omega\sqrt{\mu_o \varepsilon_2} \qquad (2.11)$$

In Fig. 3 we show the equivalent network for this external impedance. Note that the terminating element Z_i is the impedance of the center conductor while the shunt

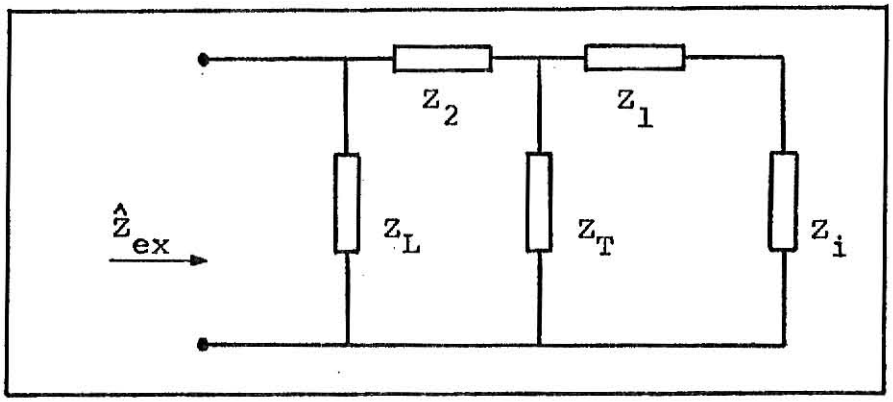

Fig. 3 The Equivalent Network for Wait's Model

elements Z_T and Z_L are the transfer impedances of the braid and the external lossy film. Z_1 and Z_2 as given in (2.10), (2.11) depend on the properties of the two dielectric layers.

2.4 Casey's model for shield; $\hat{Z}_{ex}(h)$

The analysis for the cable model which was introduced in the first section of this chapter has been done by K.F.Casey[6]. He reached an expression for the external impedance of the cable, which is

$$\hat{Z}_{ex}(h) = Z_2 + \frac{(Z_1 + Z_i)(Z_{sw} + Z_g)}{Z_1 + Z_i + Z_{sw} + Z_g} \qquad (2.12)$$

where Z_1, Z_2 are given in equations (2.10), (2.11) respect-

ively.

$$Z_q = -\frac{j\omega\mu_o \sec\psi \ln(1-e^{-\pi c_o/2})}{4\pi M} - \frac{h^2 \cos\psi \ln(1-e^{-\pi c_o/2})}{4\pi M j\omega\varepsilon_a} \qquad (2.13)$$

$$\text{and} \quad Z_{sw} = \frac{Z_w \sec^2\psi}{2M} \qquad (2.14)$$

where c_o is the optical coverage of the shield, and 2M is the number of the helices of shield wires. Furthermore,

$$\varepsilon_a = \tfrac{1}{2}(\varepsilon_1 + \varepsilon_2)$$

and Z_w denotes the impedance per unit length of shield wire. The equivalent network of this external impedance is shown in Fig. 4.

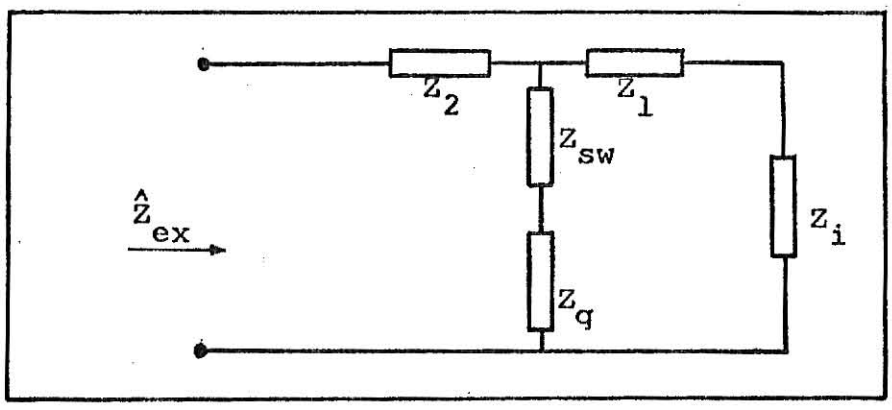

Fig. 4 The Equivalent Network for Casey's Model

Compare this result with the equivalent network from Wait as shown in Fig. 3. We may appreciate the differences

between these two models. In Casey's model, the outer lossy film has been ignored, so Z_L is infinite. Furthermore, the shunt element representing the shield differs from that of Wait. Casey's results show that the capacitive coupling of this cable is important, especially when the optical coverage c_o is small (i.e., when the cable is sparsely shielded). The effect of the capacitive coupling is expressed in the last term of equation (2.13). That is h^2/Y_s, where

$$Y_s = - \frac{4\pi M j\omega \varepsilon_a \sec\psi}{\ln(1-e^{-\pi c_o/2})} \qquad (2.15)$$

The shunt impedance $Z_{sw}+Z_q$ in Fig. 4 can be expressed equivalently as

$$Z_{sw} + Z_q = Z_s + h^2/Y_s \qquad (2.16)$$

where $$Z_s = - \frac{j\omega\mu_o \sec\psi \ln(1-e^{-\pi c_o/2})}{4\pi M} + Z_{sw} \qquad (2.17)$$

The equivalent network in Fig. 4 becomes

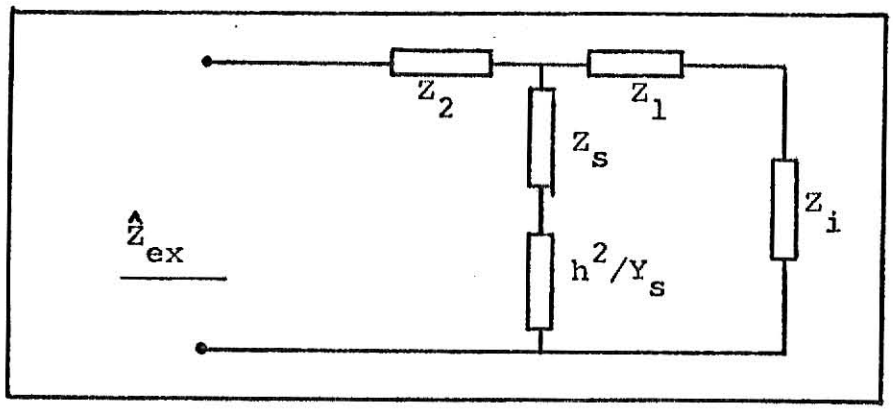

Fig. 5

Note that if Y_s goes to infinity in this model; i.e., if the capacitive coupling becomes small; then this network is the same as Wait's model in Fig. 3, and Z_s is equivalent to Z_T.

The other two transmission-line parameters Y_c, and Z_c are derived by Casey also; they are

$$Y_c = \frac{2\pi j\omega\epsilon_1}{\ln(\rho_1/r)} \qquad (2.18)$$

$$Z_c = \frac{j\omega\mu_o}{2\pi}\ln\frac{\rho_1}{r} + Z_i \qquad (2.19)$$

His final result for the external impedance $\hat{Z}_{ex}(h)$ expressed in terms of the transmission-line parameters is

$$\hat{Z}_{ex}(h) = Z_2(h) + (Y_c+Y_s)^{-1}\frac{(h^2+Y_cZ_c)(h^2+Y_sZ_s)}{h^2+(Z_c+Z_s)(1/Y_c+1/Y_s)^{-1}} \qquad (2.20)$$

Furthermore, if we consider perfectly conducting materials for the center conductor and the shield wires; i.e., $Z_i=0$, and $Z_{sw}=Z_w=0$, then

$$Z_s = -\frac{j\omega\mu_o \sec\psi \ln(1-e^{-\pi c_o/2})}{4\pi M} \qquad (2.21)$$

$$Z_c = \frac{j\omega\mu_o}{2\pi} \ln\frac{\rho_1}{r} \qquad (2.22)$$

Substitute (2.15), (2.18), (2.21) and (2.22) into (2.20); we have

$$\hat{Z}_{ex}(h) = Z_2(h) + \frac{j(k_1^2-h^2)(\omega^2 L_s - h^2 S_s)\ln(\rho_1/r)}{2\pi\omega\epsilon_1(\omega^2 L_s - h^2 S_s) - \ln(\rho_1/r)\omega(h^2-k_1^2)} \qquad (2.23)$$

where $L_s = Z_s/j\omega$; (2.24)

$$S_s = j\omega/Y_s \qquad (2.25)$$

CHAPTER 3

THE TOTAL CURRENT ON THE CABLE

3.1 Geometry of the circular tunnel

In this chapter we shall evaluate the total current on the cable, namely I_t^c. First, we shall consider the waveguide model of the circular tunnel. The geometry of this problem is illustrated in Fig. 6.

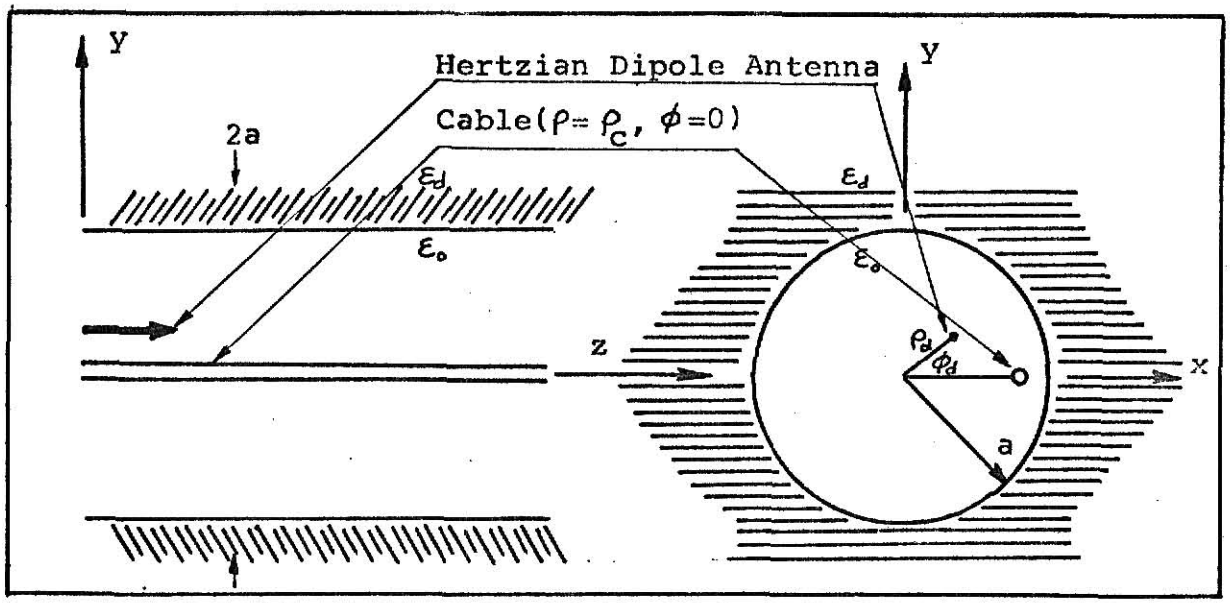

Fig. 6 The Waveguide Model of the Circular Tunnel

The tunnel radius is a while the cable is located at a distance ρ_c from the tunnel axis. There exists a Hertzian dipole source inside the tunnel at $\rho=\rho_d$, $\phi=\phi_d$. We assume that the interior region of the tunnel is free

space, and the tunnel wall material has a complex permittivity ε_d; i.e., it is a lossy dielectric material.

3.2 The expressions for Π and Φ

We may construct the field components from the Hertz potentials Π and Φ. They are solutions of the scalar Helmholtz equations:

$$(\nabla^2 + k^2) \begin{pmatrix} \Pi \\ \Phi \end{pmatrix} = 0$$

where Π yields the TM part of the field, and Φ yields the TE part of the field.

Furthermore, Π and Φ can be expressed as the inverse Fourier transforms, $\hat{\Pi}$ and $\hat{\Phi}$ respectively; here $\hat{\Pi}$ and $\hat{\Phi}$ are functions of the propagation constant $\underline{h}$.

$$\Pi(z) = \int_{-\infty}^{\infty} \hat{\Pi}(h)\, e^{-jhz}\, dh \qquad (3.1)$$

$$\Phi(z) = \int_{-\infty}^{\infty} \hat{\Phi}(h)\, e^{-jhz}\, dh \qquad (3.2)$$

or briefly, we can write

$$\begin{pmatrix} \Pi(z) \\ \Phi(z) \end{pmatrix} = \int_{-\infty}^{\infty} \begin{pmatrix} \hat{\Pi}(h) \\ \hat{\Phi}(h) \end{pmatrix} e^{-jhz}\, dh$$

It is obvious that we need appropriate forms for Π and Φ in order to construct the field components. We construct the following expressions for Π and Φ:

(1) Inside the tunnel:

$$\Pi = \Pi_d + \Pi_c + \Pi_i \quad ; \quad \Phi = \Phi_i \qquad (3.3)$$

where Π_d and Π_c are due to the dipole antenna and the cable respectively, and Π_i and Φ_i are due to the images of the dipole and the cable. We have

$$\hat{\Pi}_d = \sum_{n=-\infty}^{\infty} A_n^d \, J_n(\lambda_o \rho_{<d}) \, H_n^{(2)}(\lambda_o \rho_{>d}) \, \exp(-jn(\phi-\phi_d)) \qquad (3.4)$$

$$\hat{\Pi}_c = \sum_{n=-\infty}^{\infty} A_n^c \, J_n(\lambda_o \rho_{<c}) \, H_n^{(2)}(\lambda_o \rho_{>c}) \, \exp(-jn\phi) \qquad (3.5)$$

$$\hat{\Pi}_i = \sum_{n=-\infty}^{\infty} B_n \, J_n(\lambda_o \rho) \, \exp(-jn\phi)$$

$$\hat{\Phi}_i = \sum_{n=-\infty}^{\infty} D_n \, J_n(\lambda_o \rho) \, \exp(-jn\phi)$$

where A_n^d, A_n^c, B_n and D_n are constants to be determined. Furthermore,

$$\rho_{<d} = \min(\rho, \rho_d) \quad ; \quad \rho_{>d} = \max(\rho, \rho_d)$$

$$\rho_{<c} = \min(\rho, \rho_c) \quad ; \quad \rho_{>c} = \max(\rho, \rho_c)$$

$$\lambda_0^2 = k_0^2 - h^2 \qquad ; \qquad k_0^2 = \omega^2 \mu_o \varepsilon_o$$

(2) Outside the tunnel:

Similarly, for Ψ and Φ outside the tunnel, we have

$$\Psi = \Psi_0 \qquad ; \qquad \Phi = \Phi_0 \qquad \text{——————————} \qquad (3.6)$$

$$\hat{\Psi}_0 = \sum_{n=-\infty}^{\infty} C_n \, H_n^{(2)}(\lambda_d \rho) \exp(-jn\phi) \qquad \text{——————————} \qquad (3.7)$$

$$\hat{\Phi}_0 = \sum_{n=-\infty}^{\infty} E_n \, H_n^{(2)}(\lambda_d \rho) \exp(-jn\phi) \qquad \text{——————————} \qquad (3.8)$$

where C_n and E_n are constants. Also,

$$\lambda_d^2 = k_d^2 - h^2 \qquad ; \qquad k_d^2 = \omega^2 \mu_o \varepsilon_d$$

3.3 The boundary conditions on the tunnel wall

Now, suppose A_n^d and A_n^c are known; we want to solve B_n and D_n in terms of them, so that the field components can be found inside the tunnel. For doing this, we must use the boundary conditions that the tangential E field and tangential H field are continuous on the tunnel wall.

Firstly, the E field and H field relate to Ψ and Φ as follows:

$$\bar{E} = -\nabla \times \Phi\, \bar{a}_z + \frac{1}{j\omega\epsilon} \nabla \times \nabla \times \Psi\, \bar{a}_z$$

$$\bar{H} = \nabla \times \Psi\, \bar{a}_z + \frac{1}{j\omega\mu} \nabla \times \nabla \times \Phi\, \bar{a}_z$$

After some vector operations, we reach the following equations for the field components.

$$E_\phi = \frac{\partial \Phi}{\partial \rho} + \frac{1}{j\omega\epsilon\rho} \frac{\partial^2 \Psi}{\partial \phi \partial z} \qquad (3.9)$$

$$E_z = \frac{1}{j\omega\epsilon} (k^2 + \frac{\partial^2}{\partial z^2}) \Psi \qquad (3.10)$$

$$H_\phi = \frac{1}{j\omega\mu\rho} \frac{\partial^2 \Phi}{\partial \phi \partial z} - \frac{\partial \Psi}{\partial \rho} \qquad (3.11)$$

$$H_z = \frac{1}{j\omega\mu} (k^2 + \frac{\partial^2}{\partial z^2}) \Phi \qquad (3.12)$$

Consider the case where $a > \rho > \rho_c > \rho_d$; then equations (3.4) and (3.5) become

$$\hat{\Psi}_d = \sum_{n=-\infty}^{\infty} A_n^d J_n(\lambda_o \rho_d)\, H_n^{(2)}(\lambda_o \rho)\, \exp(-jn(\phi - \phi_d))$$

$$\hat{\Psi}_c = \sum_{n=-\infty}^{\infty} A_n^c J_n(\lambda_o \rho_c)\, H_n^{(2)}(\lambda_o \rho)\, \exp(-jn\phi)$$

So, from equations (3.1) and (3.2)

$$\Psi_d = \int_{-\infty}^{\infty} \hat{\Psi}_d e^{-jhz} dh = \int_{-\infty}^{\infty} \sum_{-\infty}^{\infty} A_n^d J_n(\lambda_0 \rho_d) H_n^{(2)}(\lambda_0 \rho) \exp(-jn(\phi - \phi_d)) \exp(-jhz) dh$$

$$\Psi_c = \int_{-\infty}^{\infty} \hat{\Psi}_c e^{-jhz} dh = \int_{-\infty}^{\infty} \sum_{-\infty}^{\infty} A_n^c J_n(\lambda_0 \rho_c) H_n^{(2)}(\lambda_0 \rho) \exp(-jn\phi) \exp(-jhz) dh$$

$$\Psi_i = \int_{-\infty}^{\infty} \hat{\Psi}_i e^{-jhz} dh = \int_{-\infty}^{\infty} \sum_{-\infty}^{\infty} B_n J_n(\lambda_0 \rho) \exp(-jn\phi) \exp(-jhz) dh$$

$$\Phi_i = \int_{-\infty}^{\infty} \hat{\Phi}_i e^{-jhz} dh = \int_{-\infty}^{\infty} \sum_{-\infty}^{\infty} D_n J_n(\lambda_0 \rho) \exp(-jn\phi) \exp(-jhz) dh$$

Then from equation (3.3)

$$\Psi = \int_{-\infty}^{\infty} \sum_{-\infty}^{\infty} [A_n^d J_n(\lambda_0 \rho_d) H_n^{(2)}(\lambda_0 \rho) \exp(jn\phi_d) + A_n^c J_n(\lambda_0 \rho_c) H_n^{(2)}(\lambda_0 \rho) + B_n J_n(\lambda_0 \rho)] \exp[-j(n\phi + hz)] dh \quad \text{---------- (3.13)}$$

$$\Phi = \Phi_i = \int_{-\infty}^{\infty} \sum_{-\infty}^{\infty} D_n J_n(\lambda_0 \rho) \exp[-j(n\phi + hz)] dh \quad \text{---------- (3.14)}$$

Substitute (3.13), (3.14) into (3.9). After perfoming some straightforward algebraic manipulations, we reach the following expression for E_ϕ:

$$E_\phi = \int_{-\infty}^{\infty} \sum_{-\infty}^{\infty} [D_n \lambda_0 J_n'(\lambda_0 \rho) - \frac{1}{j\omega\epsilon_o \rho} hn \hat{\hat{\Psi}}^i] \exp[-j(n\phi + hz)] dh$$

where $$\hat{\hat{\Psi}}^i = [A_n^d J_n(\lambda_0 \rho_d) H_n^{(2)}(\lambda_0 \rho) \exp(jn\phi_d) + A_n^c J_n(\lambda_0 \rho_c) H_n^{(2)}(\lambda_0 \rho) + B_n J_n(\lambda_0 \rho)]$$

or, we may write in a more efficient form

$$E_\phi(\rho,\phi,z) = \sum_{-\infty}^{\infty}\int_{-\infty}^{\infty}\hat{E}_{\phi n}(h)\exp[-j(n\phi+hz)]\,dh$$

where $$\hat{E}_{\phi n}(h) = D_n\lambda_o J_n'(\lambda_o\rho) - \frac{1}{j\omega\varepsilon_o\rho}\,hn\hat{\hat{\Phi}}^i$$

Similar results can be obtained for E_z, H_ϕ, and H_z from equations (3.10) (3.11) (3.12) (3.13) and (3.14). We may make a summary of these results:

When $a>\rho>\rho_c>\rho_d$, we have

$$\begin{bmatrix}E_\phi(z)\\E_z(z)\\H_\phi(z)\\H_z(z)\end{bmatrix} = \sum_{-\infty}^{\infty}\int_{-\infty}^{\infty}\begin{bmatrix}\hat{E}_{\phi n}(h)\\\hat{E}_{zn}(h)\\\hat{H}_{\phi n}(h)\\\hat{H}_{zn}(h)\end{bmatrix}\exp[-j(n\phi+hz)]\,dh$$

where $$\hat{E}_{\phi n}(h) = D_n\lambda_o J_n'(\lambda_o\rho) - \frac{1}{j\omega\varepsilon_o\rho}\,hn\hat{\hat{\Phi}}^i \qquad (3.15)$$

$$\hat{E}_{zn}(h) = -\left(j\omega\mu_o + \frac{h^2}{j\omega\varepsilon_o}\right)\hat{\hat{\Phi}}^i$$

$$\hat{H}_{\phi n}(h) = -\frac{1}{j\omega\mu_o\rho}\,hn\hat{\hat{\Phi}}^i - [A_n^d J_n(\lambda_o\rho_d)\lambda_o H_n^{(2)'}(\lambda_o\rho)\exp(jn\phi_d) + A_n^c J_n(\lambda_o\rho_c)\lambda_o H_n^{(2)'}(\lambda_o\rho) + B_n\lambda_o J_n'(\lambda_o\rho)]$$

$$\hat{H}_{zn}(h) = -\left(j\omega\varepsilon_o + \frac{h^2}{j\omega\mu_o}\right)\hat{\hat{\Phi}}^i$$

and $$\hat{\hat{\Phi}}^i = [A_n^d J_n(\lambda_o\rho_d)H_n^{(2)}(\lambda_o\rho)\exp(jn\phi_d) + A_n^c J_n(\lambda_o\rho_c)H_n^{(2)}(\lambda_o\rho) + B_n J_n(\lambda_o\rho)]$$

$$\hat{\hat{\Phi}}^{i} = D_n J_n(\lambda_o \rho)$$

Next, consider the case where $\rho > a$; by equations (3.6)—(3.8) and (3.9)—(3.12) we have the following results:

$$\begin{bmatrix} E_\phi(z) \\ E_z(z) \\ H_\phi(z) \\ H_z(z) \end{bmatrix} = \sum_n \int_{-\infty}^{\infty} \begin{bmatrix} \hat{E}_{\phi n}(h) \\ \hat{E}_{zn}(h) \\ \hat{H}_{\phi n}(h) \\ \hat{H}_{zn}(h) \end{bmatrix} \exp[-j(n\phi + hz)]\, dh$$

where $$\hat{E}_{\phi n}(h) = E_n \lambda_d H_n^{(2)'}(\lambda_d \rho) - \frac{1}{j\omega\varepsilon_d \rho} hn \hat{\hat{\Phi}}^{o} \qquad (3.16)$$

$$\hat{E}_{zn}(h) = -\left(j\omega\mu_d + \frac{h^2}{j\omega\varepsilon_d}\right)\hat{\hat{\Phi}}^{o}$$

$$\hat{H}_{\phi n}(h) = -\frac{1}{j\omega\mu_d \rho} hn \hat{\hat{\Phi}}^{o} - C_n \lambda_d H_n^{(2)'}(\lambda_d \rho)$$

$$\hat{H}_{zn}(h) = -\left(j\omega\varepsilon_d + \frac{h^2}{j\omega\mu_d}\right)\hat{\hat{\Phi}}^{o}$$

and $$\hat{\hat{\Phi}}^{o} = C_n H_n^{(2)}(\lambda_d \rho)$$

$$\hat{\hat{\Phi}}^{o} = E_n H_n^{(2)}(\lambda_d \rho)$$

The boundary conditions on the tunnel wall require that the tangential E field and tangential H field must

be continuous at $\rho=a$. Hence, the two expressions for $\hat{E}_{\phi n}$, equations (3.15) and (3.16), must be equal if we put $\rho=a$ in both of them; this is true also for $\hat{E}_{zn}$, $\hat{H}_{\phi n}$, and $\hat{H}_{zn}$.

Consequently, we obtain the following four equations with four unknowns B_n, C_n, D_n, and E_n.

$$D_n\lambda_o J_n'(\lambda_o a) - \frac{1}{j\omega\varepsilon_o a} hn\hat{\Phi}^i_{\rho=a} = E_n\lambda_d H_n^{(2)'}(\lambda_d a) - \frac{1}{j\omega\varepsilon_d a} hn\hat{\Phi}^o_{\rho=a}$$

$$- (j\omega\mu_o + \frac{h^2}{j\omega\varepsilon_o})\hat{\Phi}^i_{\rho=a} = - (j\omega\mu_d + \frac{h^2}{j\omega\varepsilon_d})\hat{\Phi}^o_{\rho=a}$$

$$- \frac{1}{j\omega\mu_o a} hn\hat{\Phi}^i_{\rho=a} - [A_n^d J_n(\lambda_o\rho_d)\lambda_o H_n^{(2)'}(\lambda_o a)\exp(jn\phi_d) + A_n^c J_n(\lambda_o\rho_c)$$
$$\lambda_o H_n^{(2)'}(\lambda_o a) + B_n\lambda_o J_n'(\lambda_o a)] = - \frac{1}{j\omega\mu_d a} hn\hat{\Phi}^o_{\rho=a}$$
$$- C_n\lambda_d H_n^{(2)'}(\lambda_d a)$$

$$- (j\omega\varepsilon_o + \frac{h^2}{j\omega\mu_o})\hat{\Phi}^i_{\rho=a} = - (j\omega\varepsilon_d + \frac{h^2}{j\omega\mu_d})\hat{\Phi}^o_{\rho=a}$$

Solving these equations for B_n and D_n is a tedious but straightforward algebraic operation. We obtain

$$B_n = -\{[M_{21}+P_{12}L_{11}L_{31}P_{11}/M_{11}] / [M_{12}+P_{12}L_{11}L_{11}P_{11}/M_{11}]\} A_n^d$$

$$-\{[M_{22}+P_{12}L_{11}L_{32}P_{11}/M_{11}] / [M_{12}+P_{12}L_{11}L_{11}P_{11}/M_{11}]\} A_n^c \quad (3.17)$$

$$D_n = \{P_{11}L_{11}\{M_{21}+P_{12}L_{11}L_{31}P_{11}/M_{11}\}/M_{11}\{M_{12}+P_{12}L_{11}L_{11}P_{11}/M_{11}\} - P_{11}/M_{11}L_{31}\}A_n^d + \{P_{11}L_{11}\{M_{22}+P_{12}L_{11}L_{32}P_{11}/M_{11}\}/ M_{11}\{M_{12}+P_{12}L_{11}L_{11}P_{11}/M_{11}\} - P_{11}/M_{11}L_{32}\}A_n^c$$

where $M_{21} = L_{41}-(j\omega\varepsilon_d\lambda_o^2L_{31}L_{22})/(j\omega\varepsilon_o\lambda_dL_{12})$

$M_{22} = L_{42}-(j\omega\varepsilon_d\lambda_o^2L_{32}L_{22})/(j\omega\varepsilon_o\lambda_dL_{12})$

$M_{11} = \lambda_oL_{21}-(j\omega\mu_d\lambda_o^2L_{11}L_{22})/(j\omega\mu_o\lambda_dL_{12})$

$M_{12} = \lambda_oL_{21}-(j\omega\varepsilon_d\lambda_o^2L_{11}L_{22})/(j\omega\varepsilon_o\lambda_dL_{12})$

$P_{11} = (\lambda_o^2R)/(j\omega\varepsilon_o\lambda_d^2)-R/j\omega\varepsilon_o$

$P_{12} = (\lambda_o^2R)/(j\omega\mu_o\lambda_d^2)-R/j\omega\mu_o$

$R = hn/a$

$L_{11} = J_n(\lambda_o a)$

$L_{12} = H_n^{(2)}(\lambda_d a)$

$L_{21} = J_n'(\lambda_o a)$

$$L_{22} = H_n^{(2)'}(\lambda_d a)$$

$$L_{31} = J_n(\lambda_o \rho_d) H_n^{(2)}(\lambda_o a) \exp(jn\phi_d)$$

$$L_{32} = J_n(\lambda_o \rho_c) H_n^{(2)}(\lambda_o a)$$

$$L_{41} = J_n(\lambda_o \rho_d) \lambda_o H_n^{(2)'}(\lambda_o a) \exp(jn\phi_d)$$

$$L_{42} = J_n(\lambda_o \rho_c) \lambda_o H_n^{(2)'}(\lambda_o a)$$

3.4 The total current on the cable; $I_t^c(z)$

Suppose the radius of the dipole antenna is much smaller than the radius of the tunnel; this is always true in the actual situation, as in Fig. 7.

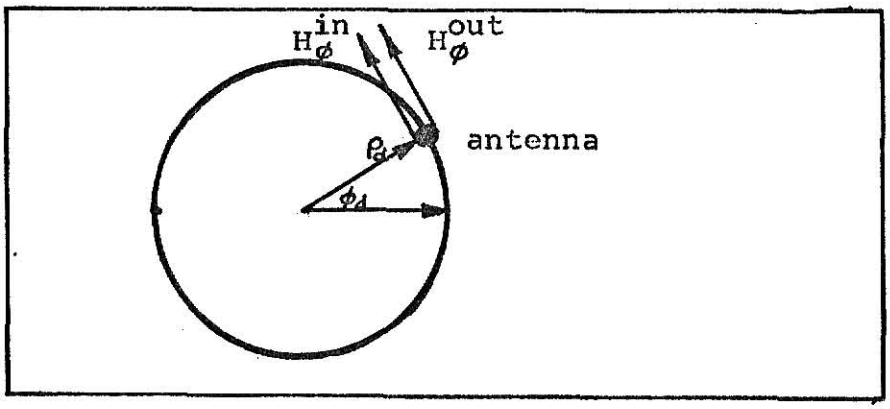

Fig. 7

Then the boundary condition for the azimuthal magnetic field H_ϕ requires that

$$H_{\phi}^{out} - H_{\phi}^{in} = J_t^d \qquad (3.18)$$

where H_{ϕ}^{out} means the azimuthal magnetic field evaluated on the dipole surface which is closer to the tunnel wall, and H_{ϕ}^{in} is the same field component on the dipole surface which is closer to the axis of the tunnel. J_t^d is the z-directional surface current density on the dipole. From equation (3.11)

$$H_{\phi} = \frac{1}{j\omega\mu\rho}\frac{\partial^2 \Phi}{\partial\phi\partial z} - \frac{\partial\Psi}{\partial\rho}$$

we have

$$H_{\phi}^{out} = \left(\frac{1}{j\omega\mu_o\rho}\frac{\partial^2}{\partial\phi\,\partial z}\Phi\right)_{\rho=\rho_d} - \left\{\frac{\partial}{\partial\rho}\int_{-\infty}^{\infty}\sum_{-\infty}^{\infty}\left[A_n^d J_n(\lambda_o\rho_d)H_n^{(2)}(\lambda_o\rho)\exp(jn\phi_d)\right.\right.$$

$$\left.\left.+A_n^c J_n(\lambda_o\rho)H_n^{(2)}(\lambda_o\rho_c)+B_n J_n(\lambda_o\rho)\right]\exp[-j(n\phi+hz)]\,dh\right\}_{\rho=\rho_d} \qquad (3.19)$$

and

$$H_{\phi}^{in} = \left(\frac{1}{j\omega\mu_o\rho}\frac{\partial^2}{\partial\phi\,\partial z}\Phi\right)_{\rho=\rho_d} - \left\{\frac{\partial}{\partial\rho}\int_{-\infty}^{\infty}\sum_{-\infty}^{\infty}\left[A_n^d J_n(\lambda_o\rho)H_n^{(2)}(\lambda_o\rho_d)\exp(jn\phi_d)\right.\right.$$

$$\left.\left.+A_n^c J_n(\lambda_o\rho)H_n^{(2)}(\lambda_o\rho_c)+B_n J_n(\lambda_o\rho)\right]\exp[-j(n\phi+hz)]\,dh\right\}_{\rho=\rho_d} \qquad (3.20)$$

Substitute (3.19) and (3.20) into (3.18); then

$$J_t^d = \left\{\frac{\partial}{\partial\rho}\int_{-\infty}^{\infty}\sum_{-\infty}^{\infty}\left[A_n^d J_n(\lambda_o\rho)H_n^{(2)}(\lambda_o\rho_d) - A_n^d J_n(\lambda_o\rho_d)H_n^{(2)}(\lambda_o\rho)\right]\exp(jn\phi_d)\right.$$
$$\left.\exp[-j(n\phi+hz)]\,dh\right\}_{\rho=\rho_d} \qquad (3.21)$$

Take the Fourier transform on both sides of equation (3.21):

$$\hat{J}_t^d = \left\{\frac{\partial}{\partial\rho}\sum_{-\infty}^{\infty}\left[A_n^d J_n(\lambda_o\rho)H_n^{(2)}(\lambda_o\rho_d) - A_n^d J_n(\lambda_o\rho_d)H_n^{(2)}(\lambda_o\rho)\right]\exp(jn\phi_d)\right.$$
$$\left.\exp(-jn\phi)\right\}_{\rho=\rho_d}$$

Hence

$$\hat{J}_t^d(h) = \sum_{-\infty}^{\infty} A_n^d \lambda_o \left[J_n'(\lambda_o\rho_d)H_n^{(2)}(\lambda_o\rho_d) - J_n(\lambda_o\rho_d)H_n^{(2)\prime}(\lambda_o\rho_d)\right]$$
$$\exp[-j(n\phi-n\phi_d)] \qquad (3.22)$$

By definition, $H_n^{(2)}(x) = J_n(x) - jN_n(x)$

$$\left[J_n'(x)H_n^{(2)}(x) - J_n(x)H_n^{(2)\prime}(x)\right] = j\left[J_n(x)N_n'(x) - J_n'(x)N_n(x)\right]$$
$$= \frac{2j}{\pi x}$$

so that equation (3.22) becomes

$$\hat{J}_t^d(h) = \sum_{-\infty}^{\infty} A_n^d \exp[-j(n\phi-n\phi_d)]\frac{2j}{\pi\rho_d}$$

so

$$\sum_{-\infty}^{\infty} A_n^d \exp[-j(n\phi - n\phi_d)] = \hat{J}_t^d(h)\ \frac{\pi \rho_d}{2j} \qquad (3.23)$$

Now, we must find the expression for $\hat{J}_t^d(h)$.

Let $\hat{J}_t^d(h) = K(h)\ \delta(\phi - \phi_d)$; where δ denotes delta function ,

then

$$\hat{I}_t^d(h) = \int_0^{2\pi} \hat{J}_t^d(h) \rho_d d\phi = \int_0^{2\pi} K(h)\ \delta(\phi - \phi_d) \rho_d d\phi = K(h) \rho_d$$

and

$$K(h) = \hat{I}_t^d(h) / \rho_d$$

so

$$\hat{J}_t^d(h) = \left[\hat{I}_t^d(h) / \rho_d\right] \delta(\phi - \phi_d) \qquad (3.24)$$

From (3.23) an d (3.24)

$$\sum_{-\infty}^{\infty} A_n^d \exp[-j(n\phi - n\phi_d)] = \hat{I}_t^d(h)\ \delta(\phi - \phi_d)\ \frac{\pi}{2j} \qquad (3.25)$$

In equation (3.25) the left hand side is the Fourier series expansion of the right hand side, and A_n^d are the coefficients:

$$A_n^d = \frac{1}{2\pi}\int_o^{2\pi} \frac{\hat{I}_t^d(h)\pi}{2j}\,\delta(\phi-\phi_d)\exp[jn(\phi-\phi_d)]\,d\phi$$

$$\text{so} \qquad A_n^d(h) = \frac{\hat{I}_t^d(h)}{4j}$$

The same procedures can be applied to the coaxial cable, and a similar result will be reached:

$$A_n^c(h) = \frac{\hat{I}_t^c(h)}{4j} \qquad \text{(3.26)}$$

In order to solve A_n^d explicitly in terms of the dipole moment $\underline{p}$ of the antenna, we argue that the dipole antenna has length $\underline{d}$ carrying uniform current I_o on it; i.e., $p=I_o d$. If we let d approach zero and I_o approach infinity, we may write

$$I_t^d(z) = p\delta(z)$$

take the Fourier transform:

$$\hat{I}_t^d(h) = \frac{1}{2\pi}\int_{-\infty}^{\infty} I_t^d(z)\exp(jhz)dz = \frac{1}{2\pi}\int_{-\infty}^{\infty} p\delta(z)\exp(jhz)dz = \frac{p}{2\pi}$$

hence, $A_n^d = \frac{p}{8\pi j}$ ——————————— (3.27)

For evaluating the total current on the coaxial cable $I_t^c(z)$, we apply the relation between I_t^c and the electric field outside the cable, that is

$$\hat{E}_z(\rho_c', 0, h) = \hat{Z}_{ex}(h)\ \hat{I}_t^c(h) \quad \text{———————} \quad (3.28)$$

$\hat{E}_z$ denotes the average axial electric field component at the outer surface of the cable. $\hat{Z}_{ex}(h)$ is the external impedance of the cable which has been introduced in Chapter 2. Here we set $\rho_c'=\rho_c-b$.

From equation (3.10)

$$E_z = \frac{1}{j\omega\varepsilon_o}(k_o^2 + \frac{\partial^2}{\partial z^2})\Pi$$

We have the expression for $\hat{E}_z$ as follows:

$$\hat{E}_z(\rho,\phi,h) = (-j\omega\mu_o - \frac{h^2}{j\omega\varepsilon_o}) \sum_{-\infty}^{\infty}[A_n^d J_n(\lambda_o\rho_d)H_n^{(2)}(\lambda_o\rho)\exp(jn\phi_d)$$

$$+A_n^c J_n(\lambda_o\rho)H_n^{(2)}(\lambda_o\rho_c)+B_n J_n(\lambda_o\rho)]\exp(-jn\phi)$$

so

$$\hat{E}_z(\rho_c', 0, h) = (-j\omega\mu_o - \frac{h^2}{j\omega\varepsilon_o}) \sum_{-\infty}^{\infty} [A_n^d J_n(\lambda_o\rho_d) H_n^{(2)}(\lambda_o\rho_c') \exp(jn\phi_d)$$

$$+A_n^c J_n(\lambda_o\rho_c') H_n^{(2)}(\lambda_o\rho_c) + B_n J_n(\lambda_o\rho_c')] \quad \text{---------- (3.29)}$$

From equations (3.28), (3.29), (3.17), (3.26) and (3.27) we have

$$\hat{Z}_{ex}(h)\hat{I}_t^c(h) = (-j\omega\mu_o - \frac{h^2}{j\omega\varepsilon_o}) \sum_{-\infty}^{\infty} [\frac{p}{8\pi j} J_n(\lambda_o\rho_d) H_n^{(2)}(\lambda_o\rho_c') \exp(jn\phi_d)$$

$$+ \frac{\hat{I}_t^c(h)}{4j} J_n(\lambda_o\rho_c') H_n^{(2)}(\lambda_o\rho_c)$$

$$- \frac{\{M_{21}+P_{12}L_{11}L_{31}P_{11}/M_{11}\}p}{\{M_{12}+P_{12}L_{11}L_{11}P_{11}/M_{11}\}8\pi j} J_n(\lambda_o\rho_c')$$

$$- \frac{\{M_{22}+P_{12}L_{11}L_{32}P_{11}/M_{11}\}\hat{I}_t^c(h)}{\{M_{12}+P_{12}L_{11}L_{11}P_{11}/M_{11}\}4j} J_n(\lambda_o\rho_c')]$$

Solve this equation for $\hat{I}_t^c(h)$:

$$\hat{I}_t^c(h) = \frac{p}{8\pi j}\{\sum_{-\infty}^{\infty} [J_n(\lambda_o\rho_d) H_n^{(2)}(\lambda_o\rho_c') \exp(jn\phi_d) - J_n(\lambda_o\rho_c')(M_{21}+$$

$$P_{12}L_{11}L_{31}P_{11}/M_{11})/(M_{12}+P_{12}L_{11}L_{11}P_{11}/M_{11})]\}/$$

$$\{[\hat{Z}_{ex}(h) j\omega\varepsilon_o/(k_o^2-h^2)] - (\frac{1}{4j}) \sum_{-\infty}^{\infty} [J_n(\lambda_o\rho_c') H_n^{(2)}(\lambda_o\rho_c) -$$

$$J_n(\lambda_o \rho_c')(M_{22}+P_{12}L_{11}L_{32}P_{11}/M_{11})/(M_{12}+P_{12}L_{11}L_{11}P_{11}/M_{11})\}\} \quad (3.30)$$

Next, to simplify this expression, we consider the tunnel wall as a perfectly conducting material, so that $|\varepsilon_d| \to \infty$, $|\lambda_d| \to \infty$ and

$$M_{21} \simeq - \frac{\lambda_o^2 \sqrt{\varepsilon_d}}{j\omega\varepsilon_o\sqrt{\mu_o}} L_{31}$$

$$P_{12} \simeq - \frac{hn}{aj\omega\mu_o}$$

$$P_{11} \simeq - \frac{hn}{aj\omega\varepsilon_o}$$

$$M_{11} \simeq \lambda_o L_{21}$$

$$M_{12} \simeq - \frac{\lambda_o^2 \sqrt{\varepsilon_d}}{j\omega\varepsilon_o\sqrt{\mu_o}} L_{11}$$

Hence

$$\frac{M_{21}+P_{12}L_{11}L_{31}P_{11}/M_{11}}{M_{12}+P_{12}L_{11}L_{11}P_{11}/M_{11}} \simeq L_{31}/L_{11} \quad \text{---------- (3.31)}$$

and similarly,

$$\frac{M_{22}+P_{12}L_{11}L_{32}P_{11}/M_{11}}{M_{12}+P_{12}L_{11}L_{11}P_{11}/M_{11}} \simeq L_{32}/L_{11} \quad \text{---------- (3.32)}$$

Substitute (3.31) and (3.32) into (3.30); we have

$$\hat{I}_t^c(h) = \frac{p}{8\pi j}\{F(h)/(\hat{Z}_{ex}(h)-G(h))\} \qquad (3.33)$$

where

$$F(h) = [(k_o^2-h^2)/j\omega\varepsilon_o]\sum_{-\infty}^{\infty}[J_n(\lambda_o\rho_d)H_n^{(2)}(\lambda_o\rho_c')-J_n(\lambda_o\rho_c')J_n(\lambda_o\rho_d)$$

$$H_n^{(2)}(\lambda_o a)/J_n(\lambda_o a)]\exp(jn\phi_d)$$

$$G(h) = (1/4j)[(k_o^2-h^2)/j\omega\varepsilon_o]\sum_{-\infty}^{\infty}[J_n(\lambda_o\rho_c')H_n^{(2)}(\lambda_o\rho_c)-J_n(\lambda_o\rho_c')$$

$$J_n(\lambda_o\rho_c)H_n^{(2)}(\lambda_o a)/J_n(\lambda_o a)] \qquad (3.34)$$

From (3.33) we have

$$I_t^c(z) = \frac{p}{8\pi j}\int_{-\infty}^{\infty}[F(h)/(\hat{Z}_{ex}(h)-G(h))]\exp(-jhz)dh \qquad (3.35)$$

3.5 The evaluation of I_t^c

We have expressed the total current on the cable I_t^c in an integral form as equation (3.35). To evaluate this integral, we must find the poles of the integrand, and then calculate the residues of the integrand at these poles. To find the poles, we must find the roots of the equation $\hat{Z}_{ex}(h)-G(h)=0$. From equation (3.34)

$$G(h) = (1/4j)\left[(k_o^2-h^2)/j\omega\varepsilon_o\right]\sum_{-\infty}^{\infty}\left[J_n(\lambda_o\rho_c')/J_n(\lambda_o a)\right]\left[H_n^{(2)}(\lambda_o\rho_c)\right.$$

$$\left.J_n(\lambda_o a)-J_n(\lambda_o\rho_c)H_n^{(2)}(\lambda_o a)\right]$$

Since $J_{-n}= (-1)^n J_n$ and $H_{-n}^{(2)}= (-1)^n H_n^{(2)}$,

$$G(h) =\left[(h^2-k_o^2)/4\omega\varepsilon_o\right]\left\{\left[J_o(\lambda_o\rho_c')/J_o(\lambda_o a)\right]\left[H_o^{(2)}(\lambda_o\rho_c)J_o(\lambda_o a)\right.\right.$$

$$\left.-J_o(\lambda_o\rho_c)H_o^{(2)}(\lambda_o a)\right] +2\sum_{-\infty}^{\infty}\left[J_n(\lambda_o\rho_c')/J_n(\lambda_o a)\right]\left[H_n^{(2)}(\lambda_o\rho_c)\right.$$

$$\left.\left.J_n(\lambda_o a)-J_n(\lambda_o\rho_c)H_n^{(2)}(\lambda_o a)\right]\right\}$$

Substitute $J_n(x)-jN_n(x)$ for $H_n^{(2)}(x)$; we have

$$G(h) =\left\{(h^2-k_o^2)/4\omega\varepsilon_o\right\}\left\{j\left[J_o(\lambda_o\rho_c')/J_o(\lambda_o a)\right]\left[J_o(\lambda_o\rho_c)N_o(\lambda_o a)\right.\right.$$

$$\left.-J_o(\lambda_o a)N_o(\lambda_o\rho_c)\right] +2j\sum_{n=1}^{\infty}\left[J_n(\lambda_o\rho_c')/J_n(\lambda_o a)\right]\left[J_n(\lambda_o\rho_c)\right.$$

$$\left.\left.N_n(\lambda_o a)-J_n(\lambda_o a)N_n(\lambda_o\rho_c)\right]\right\}$$

For large n, the summand $\left[J_n(\lambda_o\rho_c')/J_n(\lambda_o a)\right]\left[J_n(\lambda_o\rho_c)N_n(\lambda_o a)-\right.$ $\left.J_n(\lambda_o a)N_n(\lambda_o\rho_c)\right]$ can be approximated by $(1/n\pi)\left[(\rho_c'/\rho_c)^n-\right.$ $\left.(\rho_c'\rho_c/a^2)^n\right]$

then

$$\sum_{n=1}^{\infty}[J_n(\lambda_o\rho_c')/J_n(\lambda_o a)][J_n(\lambda_o\rho_c)N_n(\lambda_o a)-J_n(\lambda_o a)N_n(\lambda_o\rho_c)] =$$

$$\sum_{n=1}^{\infty}\{[J_n(\lambda_o\rho_c')/J_n(\lambda_o a)][J_n(\lambda_o\rho_c)N_n(\lambda_o a)-J_n(\lambda_o a)N_n(\lambda_o\rho_c)] -$$

$$(1/n\pi)[(\rho_c'/\rho_c)^n-(\rho_c\rho_c'/a^2)^n]\}+(1/\pi)\ln[(1-\rho_c\rho_c'/a^2)/(b/\rho_c)]$$

The summation on the right hand side will converge more rapidly than the summation on the left hand side.

$$G(h) = [(h^2-k_o^2)j/4\omega\varepsilon_o]\{[J_o(\lambda_o\rho_c')/J_o(\lambda_o a)][J_o(\lambda_o\rho_c)N_o(\lambda_o a)$$

$$-J_o(\lambda_o a)N_o(\lambda_o\rho_c)] +2\sum_{n=1}^{\infty}[(J_n(\lambda_o\rho_c')/J_n(\lambda_o a))(J_n(\lambda_o\rho_c)N_n(\lambda_o a)$$

$$-J_n(\lambda_o a)N_n(\lambda_o\rho_c))-(1/n\pi)((\rho_c'/\rho_c)^n-(\rho_c\rho_c'/a^2)^n)] +$$

$$(2/\pi)\ln(1-\rho_c\rho_c'/a^2)/(b/\rho_c)]\} \qquad (3.36)$$

As we shall see later, the roots h of $\hat{Z}_{ex}(h)-G(h)=0$ are always greater than k_o; this means that the values of λ_o which satisfy this equation must be imaginary, because $\lambda_o=(k_o^2-h^2)^{\frac{1}{2}}$, and therefore the arguments of those Bessel

functions in G(h) will be imaginary when $G(h)=\hat{Z}_{ex}(h)$ is satisfied. But to deal with the Bessel functions with imaginary argument is not easy, so we use the following relations to convert the Bessel functions with imaginary argument into the modified Bessel functions with real argument:

$$J_n(jx) = I_n(x)(-j)^{-n}$$

$$N_n(jx) = [\tfrac{2}{\pi}(j)^{-(n+1)}K_n(x) - J_n(jx)]/j$$

Then equation (3.36) will become:

$$G(h) = [(h^2-k_o^2)j/4\omega\varepsilon]\{\tfrac{2}{\pi}[I_o(\lambda'_o\rho'_c)/I_o(\lambda'_o a)][I_o(\lambda'_o a)K_o(\lambda'_o\rho_c) - I_o(\lambda'_o\rho_c)K_o(\lambda'_o a)] + 2\sum_{n=1}^{\infty}[\tfrac{2}{\pi}(I_n(\lambda'_o\rho'_c)/I_n(\lambda'_o a))(I_n(\lambda'_o a)K_n(\lambda'_o\rho_c) - I_n(\lambda'_o\rho_c)K_n(\lambda'_o a)) - (1/n\pi)((\rho'_c/\rho_c)^n - (\rho_c\rho'_c/a^2)^n)] + (2/\pi)\ln[(1-\rho_c\rho'_c/a^2)/(b/\rho_c)]\} \quad \text{(3.37)}$$

where $\lambda'_o=(h^2-k_o^2)^{\frac{1}{2}}$ is real number.

We have used ANL(Argonne National Laboratory) subroutines BESI and BESK for evaluating the values of modified Bessel functions with various order and arguments.

From equation (3.37), the equation $\hat{Z}_{ex}(h)-G(h)=0$ will become

$$Q = \sum_{n=1}^{\infty} \text{SUMMAND} + \text{ZHI} = 0 \qquad (3.38)$$

where

$$\text{SUMMAND} = \frac{2}{\pi}\left(I_n(\lambda_o'\rho_c')/I_n(\lambda_o'a)\right)\left(I_n(\lambda_o'a)K_n(\lambda_o'\rho_c)-I_n(\lambda_o'\rho_c)\right.$$

$$\left.K_n(\lambda_o'a)\right)-(1/n\pi)\left((\rho_c'/\rho_c)^n-(\rho_c\rho_c'/a^2)^n\right) \qquad (3.39)$$

$$\text{ZHI} = \frac{1}{\pi}\left[I_o(\lambda_o'\rho_c')/I_o(\lambda_o'a)\right]\left[I_o(\lambda_o'a)K_o(\lambda_o'\rho_c)-I_o(\lambda_o'\rho_c)K_o(\lambda_o'a)\right]$$

$$+ \frac{1}{\pi}\ln\left[(1-\rho_c\rho_c'/a^2)/(b/\rho_c)\right] + \hat{Z}_{ex}(h)\frac{2j\omega\varepsilon_o}{(h^2-k_o^2)} \qquad (3.40)$$

where $\hat{Z}_{ex}(h)$ is the external impedance of the cable given in equation (2.23).

We have developed two subroutine programs for calculation of the summation in equation (3.38). They are called BSUM and CSUM(APPEN), where BSUM calculates the sum of SUMMAND (equation (3.39)) from n=1 to n=NS, and CSUM finds the sum from n=NP=NS+1 to n=NN, The calling arguments of these two subroutines are

BSUM(X,RC,RCP,NS,BS)

CSUM(X,RC,RCP,NP,NN,CS)

where $X=\lambda_o' a$ is the only variable which contains the propagation constant h implicitly, and RC and RCP stand for ρ_c/a and ρ_c'/a respectively. The sum of BS and CS equals $\sum_{n=1}^{\infty}$SUMMAND for appropriately chosen integers NS and NN. Note that the parameters are all normalized with respect to the tunnel radius a, such as ρ_c/a, ρ_c'/a etc..

We develop another routine for calculating the value of $ZHI^{(APPEN)}$ (equation (3.40)). The calling arguments of this routine are

ZHI(X,RC,RCP,R1,R,KA,EP1,EP2,LSP,SSP,Z)

where

R1 = ρ_1/a

R = r/a

KA = $k_o a$

EP1= $\varepsilon_1/\varepsilon_o$

EP2= $\varepsilon_2/\varepsilon_o$

LSP= L_s

SSP= S_s

Then the equation Q=0 (equation (3.38)) can be solved by using linear interpolation as we have done in subroutine ROOT(APPEN);

ROOT(X1,X2,RC,RCP,R1,R,KA,EP1,EP2,LSP,SSP,NS,NP,NN,XROOT)

where X1 and X2 are two initial values used for approaching the root.

Finally, we shall get two roots for the equation $\hat{Z}_{ex}(h)-G(h)=0$.* They are denoted by h_1 and h_2 respectively as shown in Fig. 8, where the poles on the imaginary axis correspond to the perturbed empty waveguide modes.

3.6 The two transmission-line modes in the circular waveguide

Consider equation (3.35) which we rewrite as follows:

$$I_t^c(z) = \frac{p}{8\pi j}\int_{-\infty}^{\infty}[F(h)/(\hat{Z}_{ex}(h)-G(h))]\exp(-jhz)dh$$

---

* Actually there are an infinite number, corresponding to the two transmission-line modes plus all the waveguide modes. In this paper we are concentrating on the transmission-line modes, as these are most strongly influenced by the presence of the cable.

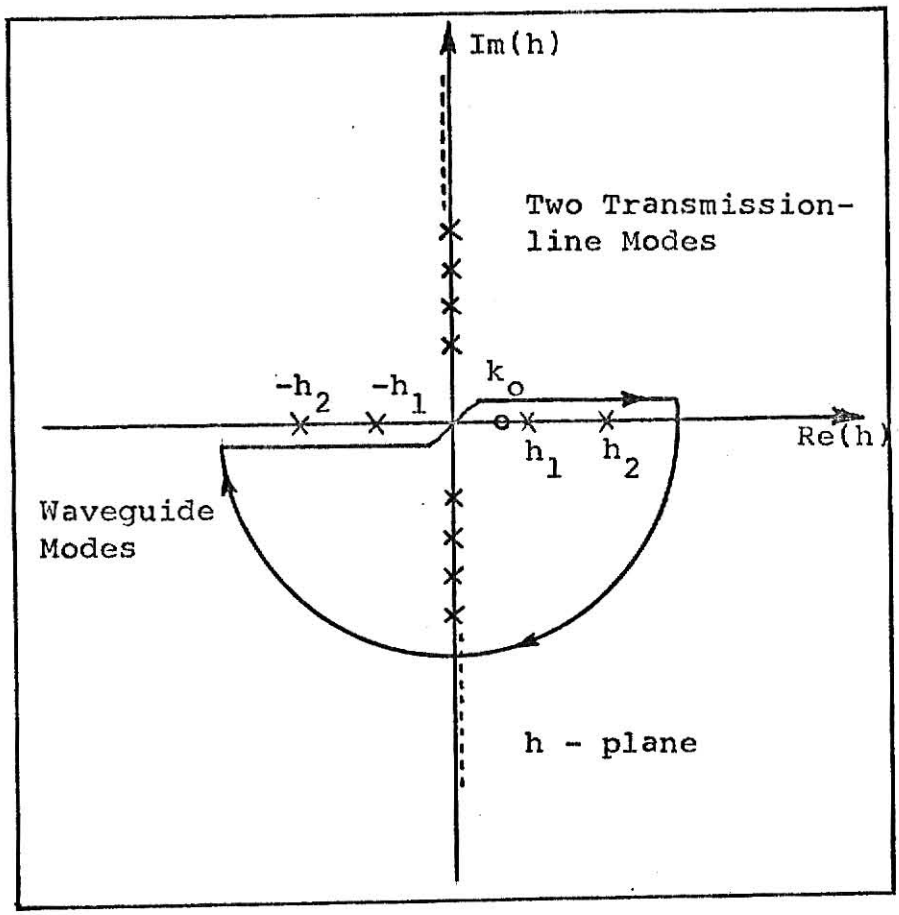

Fig. 8 The Propagation Modes in the Circular Tunnel

The integral of this integrand around the contour closed in the lower half plane will be equal to $-2\pi j$ times the sum of residues of the integrand at the poles within the contour; namely, we should have

$$\oint [F(h)/(\hat{Z}_{ex}(h)-G(h))] \exp(-jhz)dh = -2\pi j \sum \text{residues at } h_1 \text{ and } h_2 \; -2\pi j \sum \text{residues at waveguide poles} \qquad (3.41)$$

Furthermore, suppose that the frequency we consider is below the cut-off frequency of the dominant waveguide mode of this circular tunnel. Then all the waveguide modes will be attenuated rapidly with increasing z. Since for waveguide modes, the propagation constants $h_{nl} = \pm\sqrt{k_o^2 - k_{cnl}^2}$ will be pure imaginary numbers, these modes will behave like $e^{-\alpha|z|}$, where $\alpha = \sqrt{k_{cnl}^2 - k_o^2}$ is positive. As shown in Fig. 8, the poles on the imaginary axis are due to the waveguide modes of the tunnel itself perturbed by the presence of the cable. The two real poles h_1 and h_2 due to the presence of the cable correspond to the transmission-line modes which will propagate without attenuation. That is the reason we use coaxial cable for low-frequency communication inside a tunnel.

Since the contributions from the waveguide modes

can be neglected for large z, equation (3.41) can be expressed as

$$\int_{-\infty}^{\infty} + \int_{\text{C}\infty} = -2\pi j \sum \text{residues at transmission-line poles}$$

But the second integral will vanish, so we have

$$\int_{-\infty}^{\infty} [F(h)/(\hat{Z}_{ex}(h)-G(h))] \exp(-jhz)dh = -2\pi j \sum \text{residues at}$$

h_1 and h_2

and the total current on the cable I_t^c (equation (3.35)) will be

$$I_t^c(z) = \frac{p}{8\pi j}[-2\pi j \sum \text{residues at } h_1 \text{ and } h_2]$$

or

$$I_t^c(z) = -\frac{p}{4j}\left[\frac{F(h_1)\, a^2\, e^{-jh_1 z}}{\frac{a^2}{j}\frac{d}{dh}\hat{Z}_{ex}\Big|_{h=h_1} - \frac{a^2}{j}\frac{d}{dh}G\Big|_{h=h_1}} + \frac{F(h_2)\, a^2\, e^{-jh_2 z}}{\frac{a^2}{j}\frac{d}{dh}\hat{Z}_{ex}\Big|_{h=h_2} - \frac{a^2}{j}\frac{d}{dh}G\Big|_{h=h_2}}\right]$$

We have developed three routines FHK, DZH, and $DGH^{(APPEN)}$ to calculate the values of $F(h)a^2$, $\frac{a^2}{j}\frac{d}{dh}\hat{Z}_{ex}(h)$, and $\frac{a^2}{j}\frac{d}{dh}G(h)$ respectively. Then the total current is

$$I_t^c(z) = -\frac{p}{4j}\left[\frac{FHK_{h=h_1}}{DZH_{h=h_1} - DGH_{h=h_1}} e^{-jh_1 z} + \frac{FHK_{h=h_2}}{DZH_{h=h_2} - DGH_{h=h_2}} e^{-jh_2 z}\right] \qquad (3.42)$$

Equation (3.42) is our final result for the total current I_t^c; the numerical examples will be given in the next chapter. The calling arguments of subroutines FHK, DZH, and DGH are

```
FHK(XK,RD,RCP,PHID,K,NS,FH)
DZH(XK,RC,RCP,KA,A,EP1,EP2,LSP,SSP,R1,R,ZH)
DGH(XK,RC,RCP,KA,A,NS,NN,GH)
```

where $XK = \lambda'_{ok}\, a$

$\lambda'_{ok} = (h_k^2 - k_o^2)^{1/2}$ $\qquad$ $h_k = h_1$ or h_2

RD = ρ_d/a

PHID = ϕ_d

K = $k_o = \omega\sqrt{\mu_o \varepsilon_o}$

A = a

CHAPTER 4

NUMERICAL RESULTS FOR THE CABLE CURRENTS

4.1 Introduction

In the last chapter, we found that the total current on the coaxial cable is

$$I_t^c(z) = \frac{pj}{4}[I_1 e^{-jh_1 z} + I_2 e^{-jh_2 z}] \qquad (4.1)$$

where

$$I_k = \left.\frac{FHK}{DZH - DGH}\right|_{h=h_k} \qquad k=1,2$$

represents the normalized magnitude of current for the two transmission-line modes corresponding to h_1 and h_2 respectively. In the following sections, we shall investigate the dependences of I_1 and I_2 on the various parameters. The geometrical and electrical parameters of the cable are assumed to be

$r = 0.10$ cm

$\rho_1 = 0.35$ cm

$b = 0.50$ cm

$\varepsilon_1 = 2.25\ \varepsilon_o$

$\varepsilon_2 = 3.50\ \varepsilon_o$

Let the shield be constructed of (2xM) strands (M is an integer) of #36 B and S gauge Cu wire with pitch angles $\psi = \pm 25^{o}$. The radius of the tunnel is assumed to be 2.0 m .

Now consider the case M=10. We find that the optical coverage is

$c_o = 0.01275 \times M = 0.1275$; and from equations (2.21), (2.24)

$L_s = 18.8\ nHm^{-1}$; from equations (2.15), (2.25)

$S_s = 0.484\ GmF^{-1}$

4.2 The magnitude of current with respect to change of ρ_c.

First, we investigate the relations between the currents and the location of the cable. Namely, we calculate the values of currents I_1 and I_2 for different values of ρ_c with the other parameters fixed. As mentioned previously, ρ_c is the distance between the cable and the axis of the tunnel.

Assume the operating frequency is 1 MHz, so

$k_o = 0.021\ m^{-1}$; and let

$\rho_d = 0.5$ m

$\phi_d = 30^{o}$

Then the relations between I_1, I_2 and ρ_c are shown in Fig. 9. Note that I_1 is smaller than I_2. In fact, I_1, which corresponds to the bifilar mode, is the sum of the current in the center conductor and the return current in the conducting shields. So I_1 is approximately equal to zero, while I_2 corresponds to the monofilar mode which has its return current flow through the tunnel wall. Compared to I_2, we find that I_1 is almost constant with respect to changes of ρ_c. Note also that the currents decrease when the cable is moved away from the dipole source.

4.3 The magnitude of current with respect to change of ρ_d

In this section, we change the values of ρ_d rather than ρ_c. Let ρ_c equal 1.6 m, and all the other parameters except ρ_d take the same values as in section 4.2. Then we have the results for I_1 and I_2 as shown in Fig. 10 and Fig. 11 respectively. Again, note that I_1 and I_2 have a similar behavior; they all reach a maximum value at ρ_d=1.1 m, but I_1 is much smaller than I_2. In Fig. 10 and Fig. 11 we have

M = 10; c_o= 0.1275; L_s= 18.8 nHm^{-1}; S_s= 0.484 GmF^{-1}

f = 1 MHz; k_o= 0.021 m^{-1}

ρ_c= 1.6 m

ϕ_d= 30°

4.4 The magnitude of current with respect to change of ϕ_d

Fig. 12 and Fig. 13 are plots of I_1 and I_2 respectively; but this time they are functions of ϕ_d. We may expect that these curves will be symmetrical about the vertical lines ϕ_d=0 and ϕ_d=π, and the currents have maximum and minimum values at ϕ_d=0 and ϕ_d=π respectively. In Fig. 12 and Fig. 13 we have

M = 10

f = 1 MHz

ρ_c= 1.6 m

ρ_d= 0.5 m

4.5 The magnitude of current with respect to change of frequency

In Fig. 14 we show the linear relationship between I_1 and the operating frequency. We have

M = 10

ρ_d= 0.5 m

$\phi_d = 30^o$

$\rho_c = 1.6$ m

4.6 The magnitude of current with respect to change of M

Fig. 15 shows the dependence of I_1 on the values of M. As in section 4.2

$c_o = 0.01275 \times M$; and

$L_s = - 1.103 \times 10^{-7} \ln(1-e^{-\pi c_o/2})/M$

$S_s = - 2.833 \times 10^{9} \ln(1-e^{-\pi c_o/2})/M$

and in addition,

f = 1 MHz

$\rho_c = 1.6$ m

$\rho_d = 0.5$ m

$\phi_d = 30^o$

Note that when M is increased, which means that the cable is shielded more completely, the coupling from the exterior fields to the interior fields of the cable is reduced. Consequently, the current will be reduced as shown in Fig. 15.

4.7 The propagation constants h_1 and h_2

In Fig. 16, Fig. 17, and Fig. 18 we show the relationships between h_1, the propagation constant of the bifilar mode, and ρ_c, M, and frequency respectively. The propagation constant of the monofilar mode h_2 should have similar relationships with these parameters, but it is greater than h_1. Besides, we find that h_1 and h_2 do not depend on the values of ρ_d and ϕ_d.

4.8 The solutions to the transmission-line equations

After we find the total cable current $I_t^c(z)$, we are in a position to solve the transmission-line equations; i.e., equations (2.1), and (2.2)

$$\frac{dV}{dz} = - ZI - Z_s I_t^c \qquad (2.1)$$

$$\frac{dI}{dz} = - YV + j\omega \Gamma_s Q_t^c \qquad (2.2)$$

Differentiate equation (2.2) with respect to z; we have

$$\frac{dV}{dz} = j\omega \frac{\Gamma_s}{Y} \frac{dQ_t^c}{dz} - \frac{1}{Y} \frac{d^2 I}{dz^2} \qquad (4.2)$$

Substitute equation (4.2) into equation (2.1); then

$$\frac{d^2I}{dz^2} - ZYI = j\omega\Gamma_s \frac{dQ_t^c}{dz} + Z_s Y I_t^c \qquad (4.3)$$

From equations (2.3) and (4.1)

$$j\omega Q_t^c = -\frac{dI_t^c}{dz} = -\frac{p}{4}\left[h_1 I_1 e^{-jh_1 z} + h_2 I_2 e^{-jh_2 z}\right]$$

$$j\omega\frac{dQ_t^c}{dz} = +\frac{pj}{4}\left[h_1^2 I_1 e^{-jh_1 z} + h_2^2 I_2 e^{-jh_2 z}\right]$$

So equation (4.3) becomes

$$\frac{d^2I}{dz^2} - ZYI = \frac{pj}{4} I_1\left[Z_s Y + \Gamma_s h_1^2\right] e^{-jh_1 z} + \frac{pj}{4} I_2\left[Z_s Y + \Gamma_s h_2^2\right] e^{-jh_2 z} \qquad (4.4)$$

The solution of equation (4.4) can be written as

$$I = -\frac{\frac{pj}{4} I_1\left[Z_s Y + \Gamma_s h_1^2\right]}{h_1^2 + ZY} e^{-jh_1 z} - \frac{\frac{pj}{4} I_2\left[Z_s Y + \Gamma_s h_2^2\right]}{h_2^2 + ZY} e^{-jh_2 z} + C_1 e^{\sqrt{ZY}\, z} + C_2 e^{-\sqrt{ZY}\, z} \qquad (4.5)$$

where the last two terms, $C_1 e^{\sqrt{ZY}\, z}$ and $C_2 e^{-\sqrt{ZY}\, z}$, correspond to the transmission-line modes of the cable. For the case we are considering, these two terms can be ignored. So we have

$$I = -\frac{\frac{pj}{4} I_1[Z_s Y + \Gamma_s h_1^2]}{h_1^2 + ZY} e^{-jh_1 z} - \frac{\frac{pj}{4} I_2[Z_s Y + \Gamma_s h_2^2]}{h_2^2 + ZY} e^{-jh_2 z} \quad (4.6)$$

and the ratio of center conductor current to total current is

$$I/I_t^c = \frac{-\Gamma_s h_1^2 - Z_s Y}{h_1^2 + ZY} \quad \text{for the bifilar mode, and}$$

$$I/I_t^c = \frac{-\Gamma_s h_2^2 - Z_s Y}{h_2^2 + ZY} \quad \text{for the monofilar mode}$$

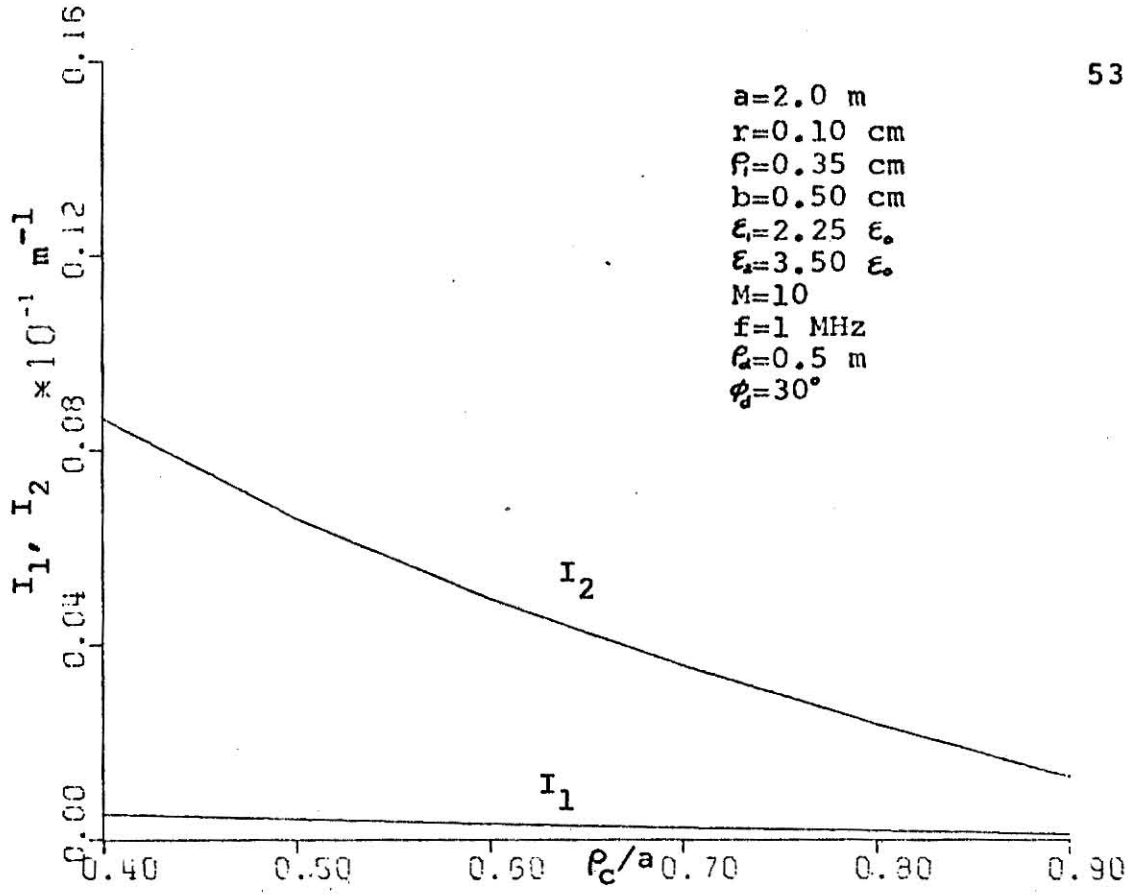

Fig. 9 I_1, I_2 vs ρ_c/a

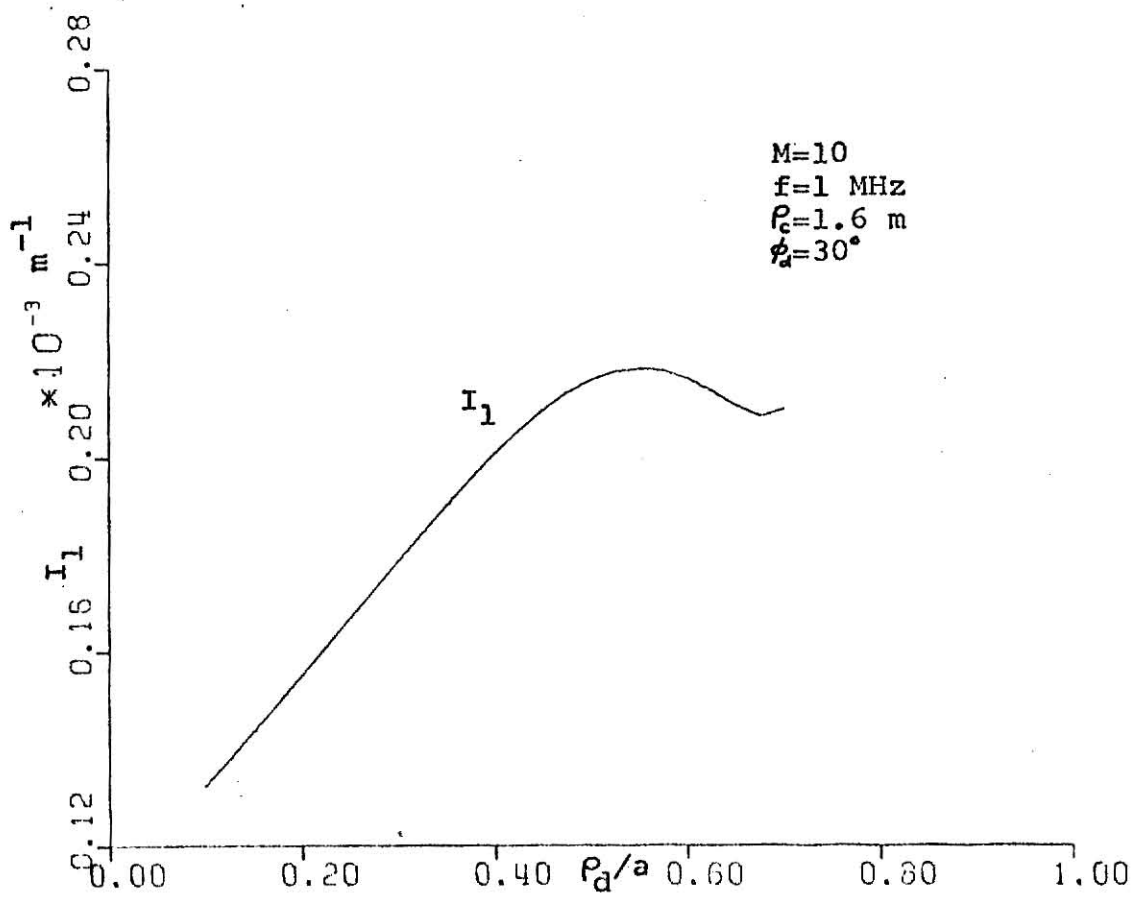

Fig. 10 I_1 vs ρ_d/a

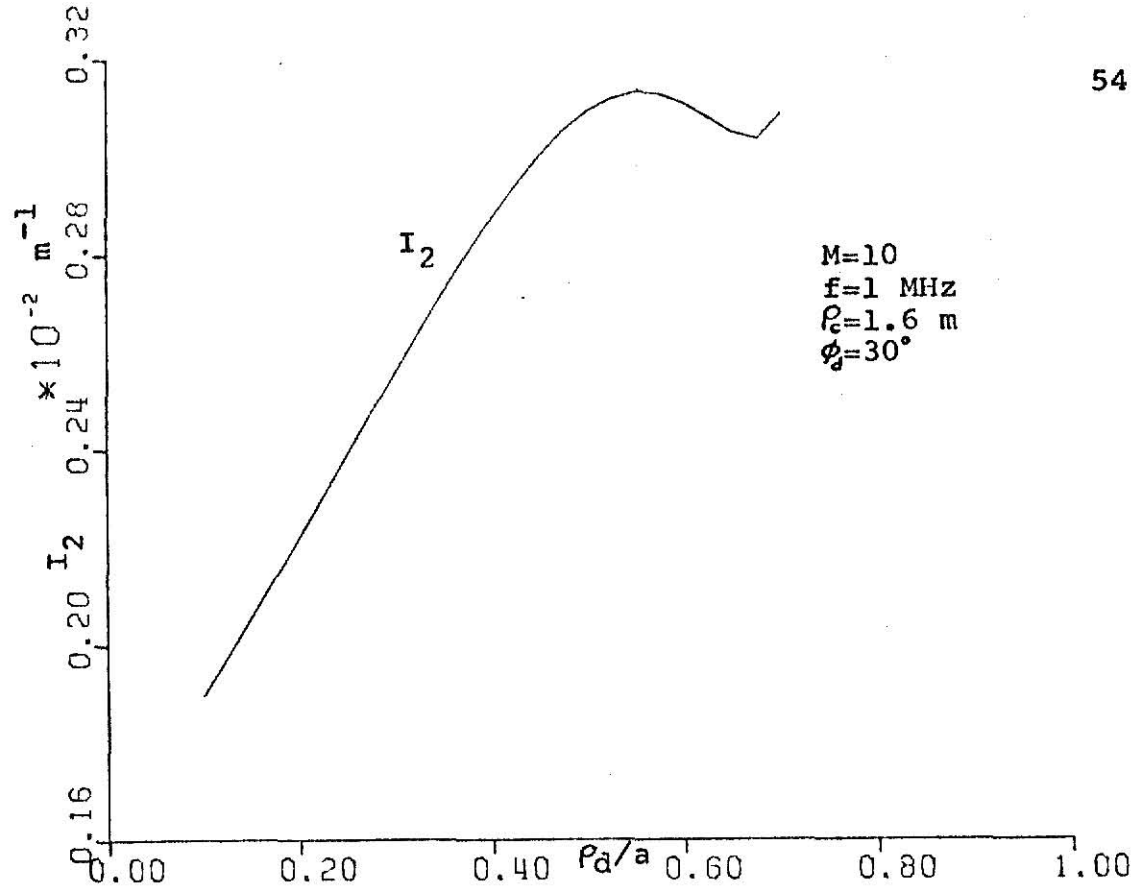

Fig. 11 I_2 vs ρ_d/a

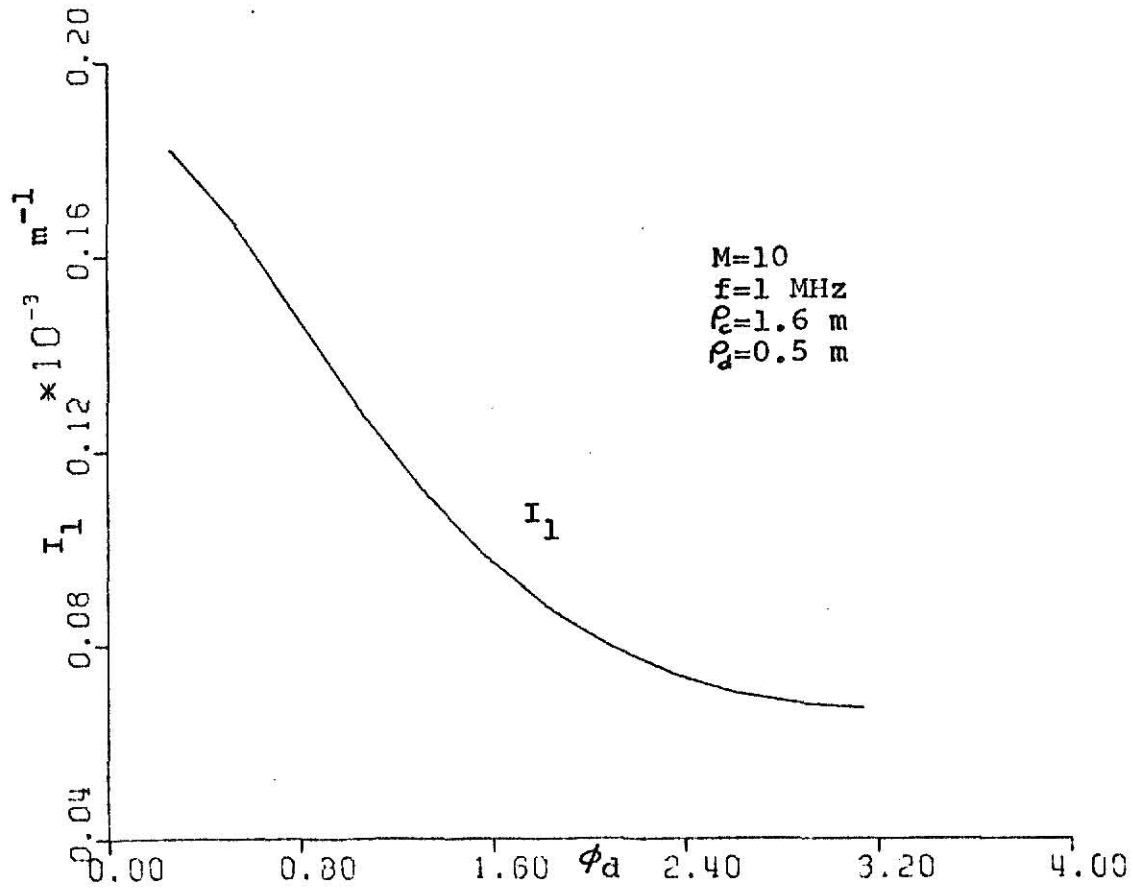

Fig. 12 I_1 vs ϕ_d

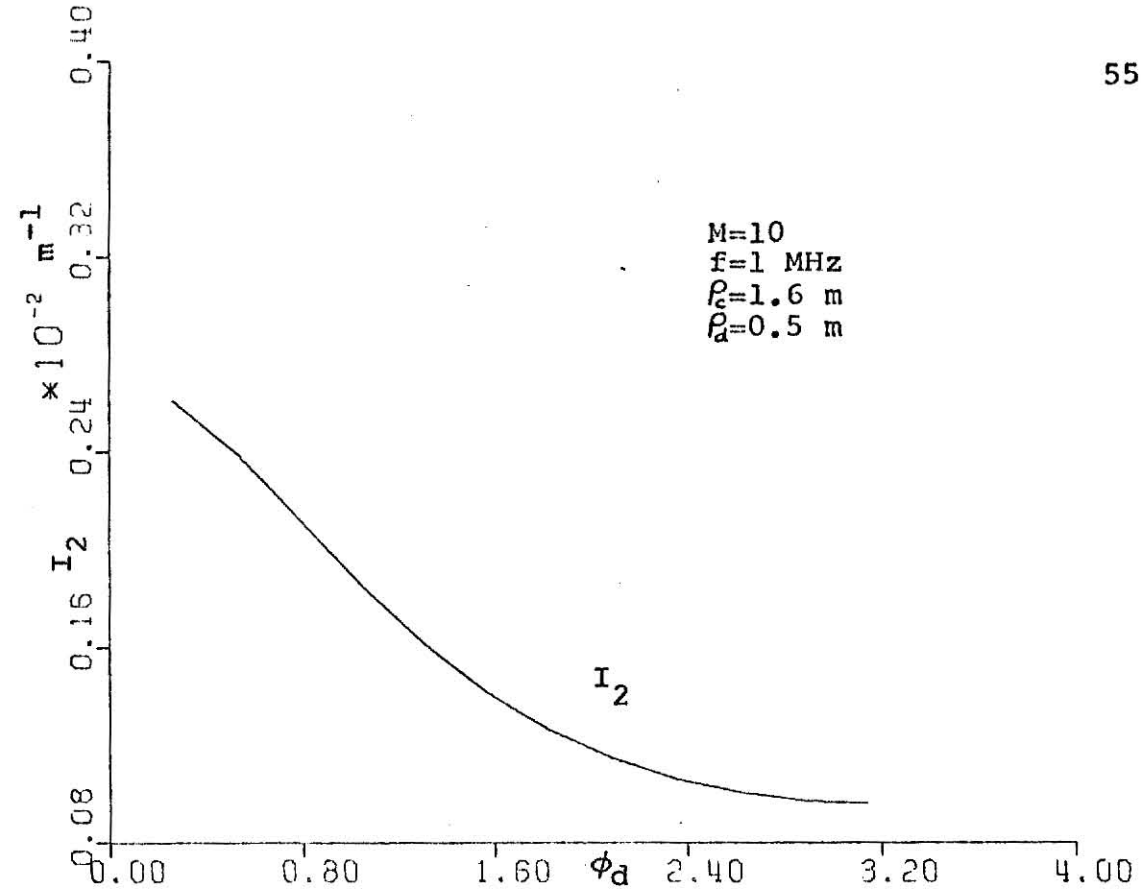

Fig. 13 I_2 vs ϕ_d

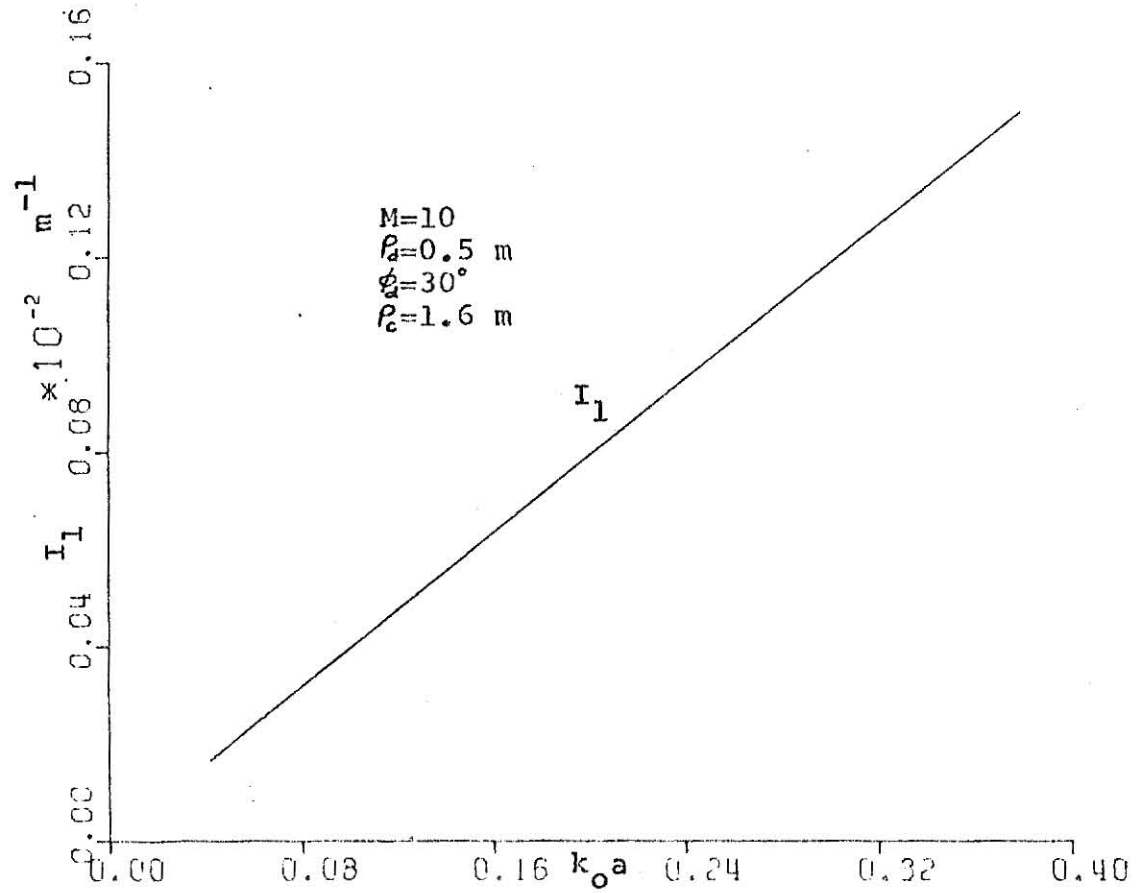

Fig. 14 I_1 vs $k_o a$

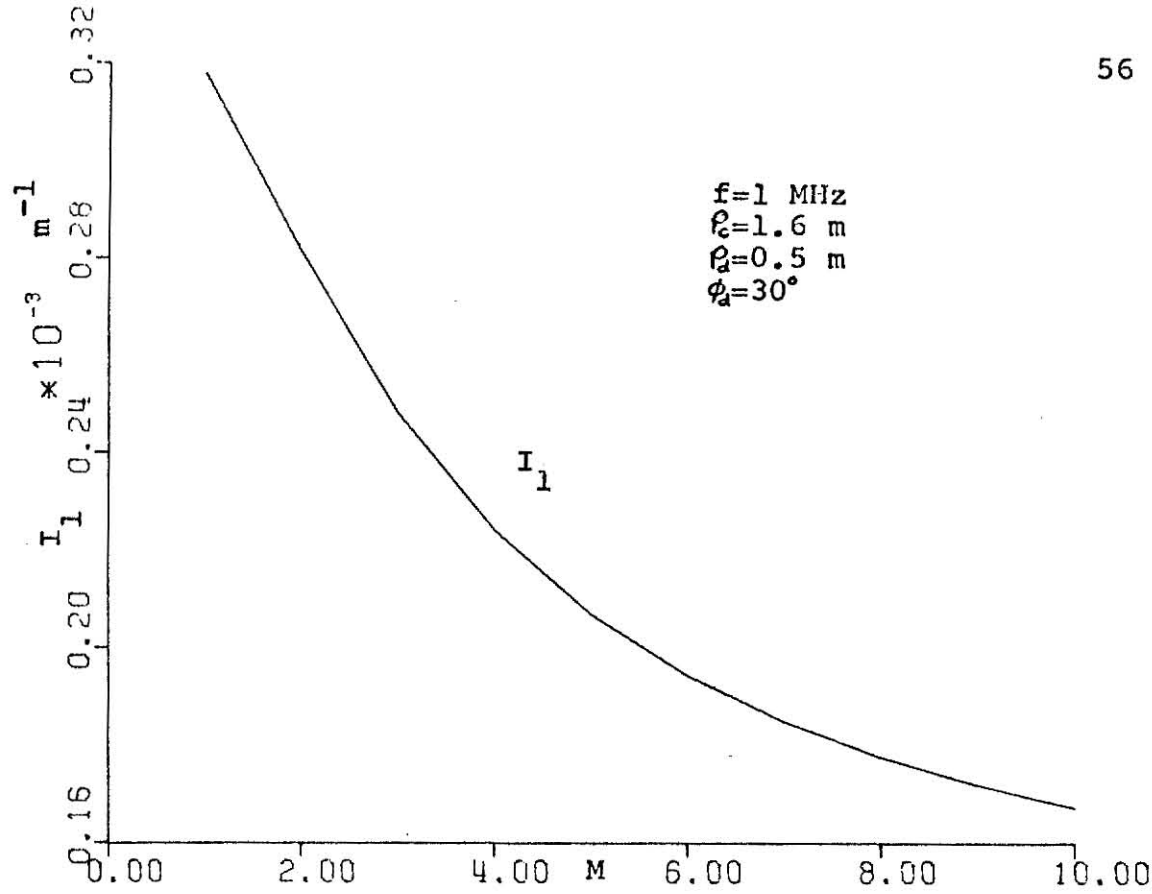

Fig. 15 I_1 vs M

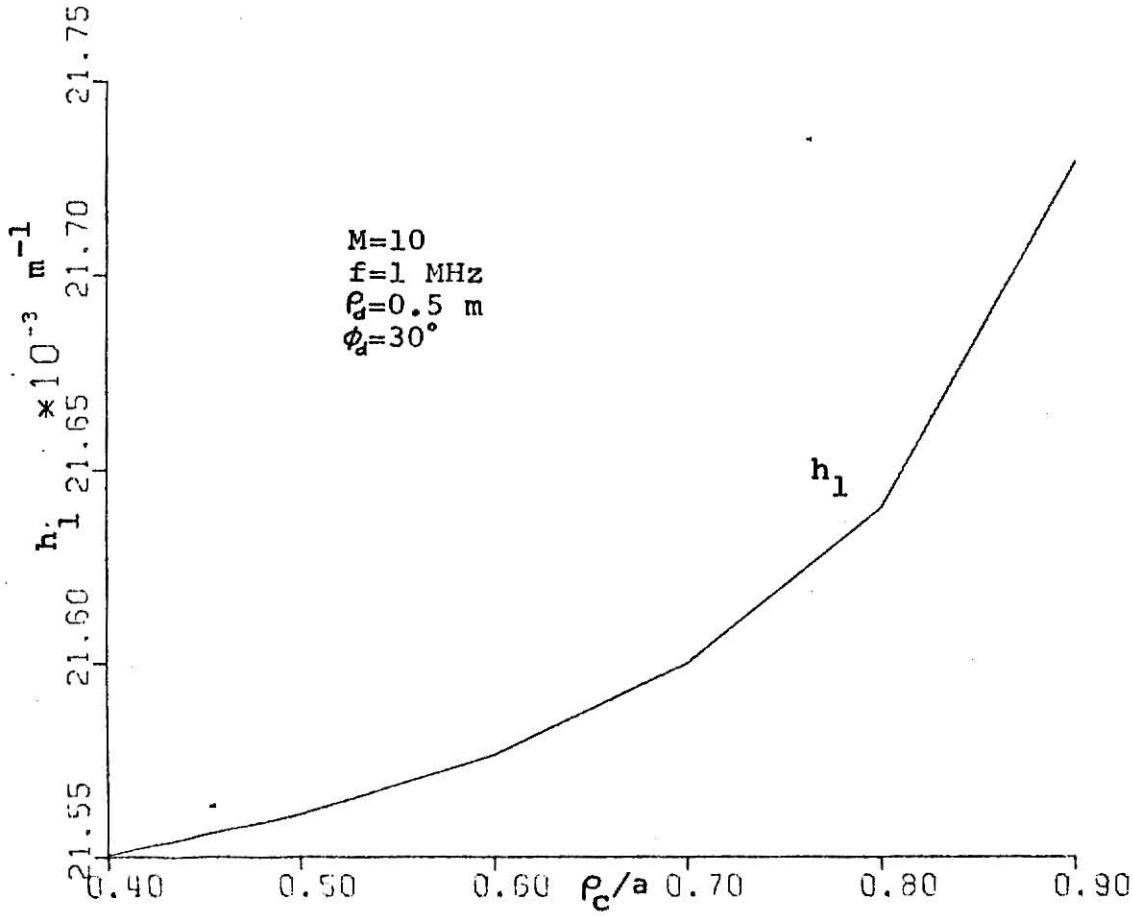

Fig. 16 h_1 vs ρ_c/a

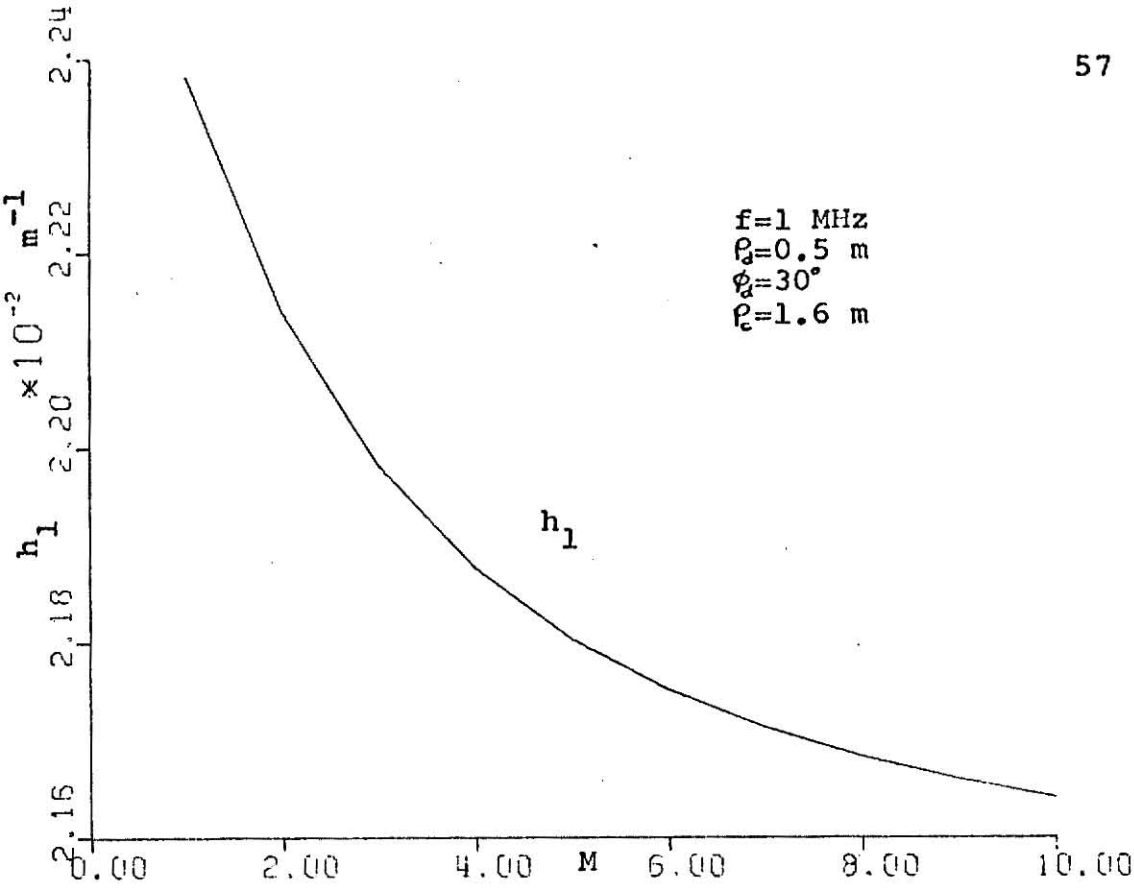

Fig. 17 h_1 vs M

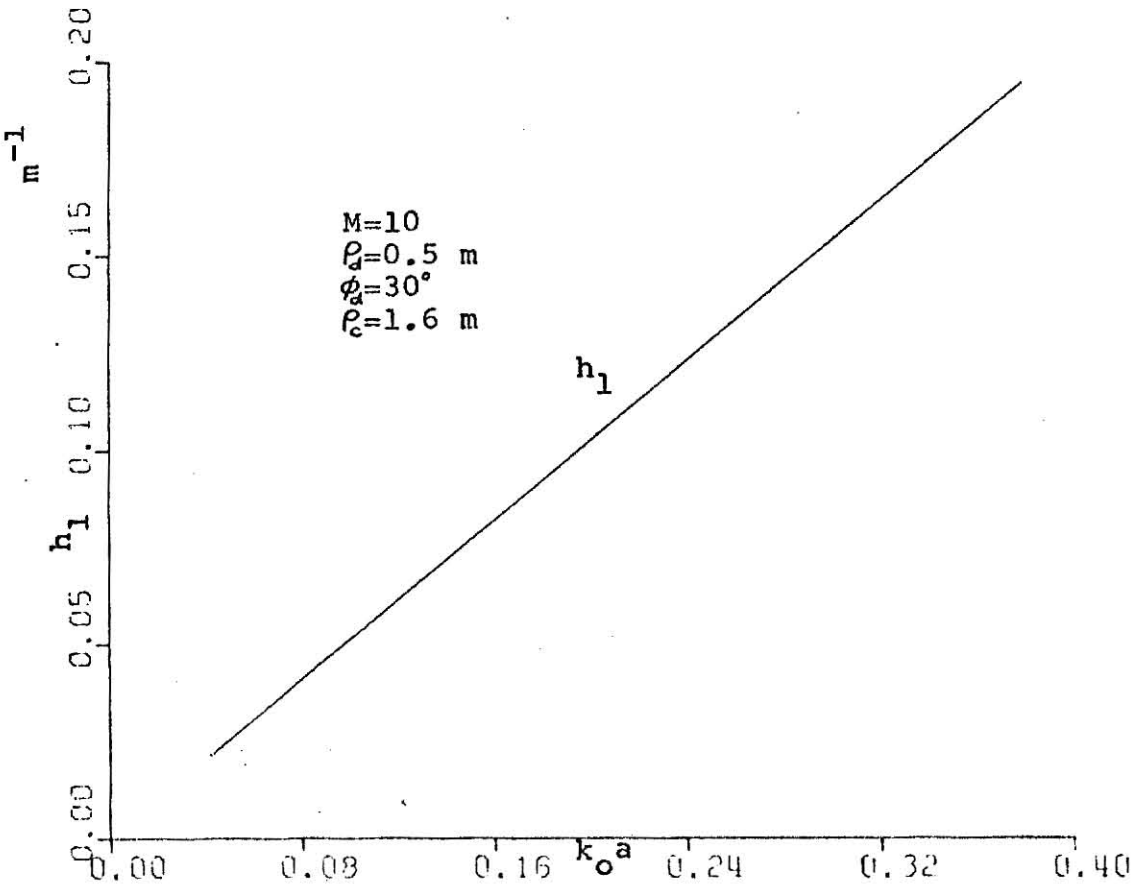

Fig. 18 h_1 vs $k_o a$

CHAPTER 5

CONCLUSIONS

The excitation and propagation of waves along a coaxial cable located within a circular tunnel have been examined in this paper. When the operating frequency is low enough such that it is below the cut-off frequency of the waveguide modes of the empty tunnel, there remain two transmission-line modes which can propagate inside the tunnel. These two modes, which due to the presence of the cable, are called the bifilar mode and the monofilar mode for obvious reasons. The bifilar mode has its return current flow in the conducting shield of the coaxial cable rather than the surrounding tunnel wall, so its attenuation rate should be small compared with that of the monofilar mode, which has its return current flow through the lossy dielectric tunnel wall.

It is obviously desirable to use the bifilar mode in long distance communication within a mine tunnel owing to its low attenuation rate. But the difficulty we have to face is the excitation problem of this bifilar mode. A very useful technique[3] has been developed for use in Belgian coal mines which is to convert

the monofilar mode, which can be excited strongly, to the bifilar mode.

The main point of this paper has been to show the existence of these two propagation modes and to illustrate their behaviors as functions of some of the parameters of the problem. We start with a model of the leaky braided-shield cable in which the capacitive as well as inductive coupling mechanisms are included. From this model an equivalent surface impedance of the cable called the external impedance can be deduced. Then we use this result to match the boundary condition on the cable surface, so we can express the cable current in terms of two components which come from the bifilar mode and the monofilar mode respectively.

As a numerical illustration, we have considered a typical coaxial cable with a perfectly conducting material as the center conductor and the shield wires. We have investigated the behaviors of the cable current when the various parameters are changed. Finally, the current on the center conductor has been found through the transmission-line equations, and the ratios of the center conductor currents to the total cable currents for the transmission-line modes have been found. Ideally this ratio for the bifilar mode should be much greater

than that for the monofilar mode, but this is probably not possible in practice.

There are two subjects beyond those considered in this paper that we may suggest for future study. The first of these is to remove the assumption of a perfectly conducting material for the tunnel wall as well as the center conductor and the shield wires of the cable. Then the attenuation rates of the two transmission-line modes can be found. The second is to neglect the capacitive coupling of the shielded coaxial cable, in order to illustrate the influence of capacitive coupling on the wave propagation problem.

ACKNOWLEDGEMENT

My sincerest thanks are extended to Dr. K.F. Casey for his direction in preparing this thesis and to the Electrical Engineering Department for the support I have received during my stay at the Kansas State University.

REFERENCES

(1) S.F. Mahmoud and J.R. Wait, " Theory of Wave propagation Along a Thin Wire Inside a Rectangular Waveguide" Radio Science, Volume 9, Number 3, pp. 417-420, March 1974

(2) J.R. Wait and D.A. Hill, " Guided Electromagnetic Waves Along an Axial Conductor in a Circular Tunnel" IEEE Transactions on Antennas and Propagation, Volume AP-22, Number 4, July 1974, pp. 627-630

(3) J.R. Wait and D.A. Hill, "Coaxial and Bifilar Modes on a Transmission Line in a Circular Tunnel" Applied Physics, Volume 4, pp. 307-312, Sept. 1974

(4) D.A. Hill and J.R. Wait, "Excitation of Monofilar and Bifilar Modes on a Transmission Line in a Circular Tunnel" Journal of Applied Physics, Volume 45, Number 8, August 1974, pp. 3402-3406

(5) J.R. Wait and D.A. Hill, "Propagation Along a Braided Coaxial Cable in a Circular Tunnel" IEEE Transactions on Microwave Theory and Techniques, Volume MIT-23, Number 5, May 1975, pp. 401-405

(6) K.F. Casey, "A Sparsely Shielded Coaxial Cable" (Unpublished Manuscript)

APPENDIX

THE FOLLOWING DOCUMENT HAS PRINTING THAT EXTENDS INTO THE BINDING.

THIS IS AS RECEIVED FROM CUSTOMER.

ILLEGIBLE DOCUMENT

THE FOLLOWING DOCUMENT(S) IS OF POOR LEGIBILITY IN THE ORIGINAL

THIS IS THE BEST COPY AVAILABLE

```
      SUBROUTINE BSUM(X,RC,RCP,NS,BS)
      REAL*8 AINA(100),AINC(100),AINCP(100),AKNA(100),AKNC(100),X,RC,RCP
     2,XRC,XRCP,DEA,DEC,DECP,T(100),BS
      PI=3.14159265358979D0-15
      XRC=X*RC
      XRCP=X*RCP
      CALL BESI(X,0.D0,NS,AINA,100)
      CALL BESI(XRC,0.D0,NS,AINC,100)
      CALL BESI(XRCP,0.D0,NS,AINCP,100)
      CALL BESK(X,0.D0,NS,AKNA,100)
      CALL BESK(XRC,0.D0,NS,AKNC,100)
      DEA=DEXP(X)
      DEC=DEXP(XRC)
      DECP=DEXP(XRCP)
      M=NS+1
      DO 1 I=2,M
    1 T(I)=((AINA(I)*AKNC(I)*AINCP(I)*DEA)/(AINA(I)*DEC)-(AINC(I)*
     2AKNA(I)*AINCP(I)*DEC)/(AINA(I)*DEA))*(DECP*2.D0)/(DEA*PI)
     3-((RCP/RC)**(I-1)-(RC*RCP)**(I-1))/((I-1)*PI)
      BS=0.D0
      DO 2 J=2,M
    2 BS=BS+T(J)
      RETURN
      END
```

```
      SUBROUTINE CSUM(X,RC,RCP,NP,NN,CS)
      REAL*8 X,RC,RCP,CS,XRC,XRCP,QA(100),QC(100),QCP(100),T(100)
      PI=3.14159265358979D-15
      XRC=X*RC
      XRCP=X*RCP
      CS=0.D0
      DO 5 N=NP,NN
      QA(N)=(N**2+X**2)**0.5
      QC(N)=(N**2+XRC**2)**0.5
      QCP(N)=(N**2+XRCP**2)**0.5
      T(N)=(1.D0/PI)*(1.D0/(QCP(N)*QC(N))**0.5)*(DEXP(QCP(N)-QC(N))*
     2((RCP*(N+QC(N)))/(RC*(N+QCP(N))))**N-DEXP(QCP(N)-2*QA(N)+QC(N))*((
     3(N+QA(N))**2/((N+QCP(N))*(N+QC(N))))*RCP*RC)**N)
     4-(1.D0/(N*PI))*((RCP/RC)**N-(RCP*RC)**N)
      CS=CS+T(N)
    5 CONTINUE
      RETURN
      END
```

```
      SUBROUTINE ZHI(X,RC,RCP,R1,R,KA,EP1,EP2,LSP,SSP,Z)
      REAL*8 X,RC,RCP,R1,R,KA,EP1,EP2,LSP,SSP,Z,PI,C,EP,ORSUM,XRC,XRCP,
     2BI(100),BIC(100),BICP(100),BK(100),BKC(100),DFA,DFC,DFCP,F1,F2,H
      PI=3.14159265358979D3
      C=2.998D8
      EP=8.854D-12
      XRC=X*RC
      XRCP=X*RCP
      DFA=DEXP(X)
      DFC=DEXP(XRC)
      DFCP=DEXP(XRCP)
      CALL BESI(X,0.D0,0,BI,100)
      CALL BESI(XRC,0.D0,0,BIC,100)
      CALL BESI(XRCP,0.D0,0,BICP,100)
      CALL BESK(X,0.D0,0,BK,100)
      CALL BESK(XRC,0.D0,0,BKC,100)
      ORSUM=(2.D0/PI)*(DFCP/DFA)*(BICP(1)/BI(1))*((DFA/DFC)*BI(1)*BKC(1)
     2-(DFC/DFA)*BIC(1)*BK(1))
      F1=X**2+KA**2*(1.D0-EP1)
      F2=X**2+KA**2*(1.D0-EP2)
      H=X**2+KA**2*(1.D0-C**2*(LSP/SSP))
      Z=0.500*ORSUM+(1.D0/PI)*DLOG((RC-RC**2*RCP)/(RC-RCP))+(F2*DLOG((RC
     2-RCP)/R1))/(PI*EP2*X**2)+(F1*H*DLOG(R1/R))/(PI*EP1*X**2*H+DLOG(R1/
     3R)*F1*(X**2/(2.D0*SSP*EP)))
      RETURN
      END
```

```
      SUBROUTINE ROOT(X1,X2,RC,RCP,P1,R,KA,EP1,EP2,LSP,SSP,NS,NP,NN,XROO
     2T)
      REAL*8 X,X1,X2,Q1,Q2,RC,RCP,BS,CS,SUM,KA,Z,XO,Q,XRCOT,P1,R,EP1,EP2
     2,LSP,SSP,QQ
      X=X1
      N=1
   10 CALL BSUM(X,RC,RCP,NS,BS)
      CALL CSUM(X,RC,RCP,NP,NN,CS)
      SUM=BS+CS
      CALL ZHI(X,RC,RCP,P1,R,KA,EP1,EP2,LSP,SSP,Z)
      IF (N.EQ.2) GO TO 20
      IF (N.EQ.0) GO TO 30
      Q1=SUM+Z
      X=X2
      N=2
      GO TO 10
   20 Q2=SUM+Z
   40 XC=(Q2*X1-Q1*X2)/(Q2-Q1)
      X=XO
      N=0
      GO TO 10
   30 Q=SUM+Z
      QQ=DABS(Q)
      IF (QQ.LT.1.0D-8) GO TO 999
      Q1=Q2
      Q2=Q
      X1=X2
      X2=X
      GO TO 40
  999 XRCOT=X
      RETURN
      END
```

```
      SUBROUTINE FHK(XK,RD,RCP,PHID,K,NS,FH)
      REAL*8 XK,FH,XRD,BI(100),BID(100),RCP,XRCP,BICP(100),BK(100),
     2BKCP(100),DFA,DFD,DFCP,PHID,PHIN,COS,PI,ST,A0,T(100),A1,Q,FH,C,
     3EP,K
      PI=3.14159265358979
      C=2.99800
      EP=8.854D-12
      XRD=XK*RD
      XRCP=XK*RCP
      DFA=DEXP(XK)
      DFD=DEXP(XRD)
      DFCP=DEXP(XRCP)
      CALL BESI(XK,0.D0,NS,BI,100)
      CALL BESI(XRD,0.D0,NS,BID,100)
      CALL BESI(XRCP,0.D0,NS,BICP,100)
      CALL BESK(XK,0.D0,NS,BK,100)
      CALL BESK(XRCP,0.D0,NS,BKCP,100)
      ST=0.D0
      NN=NS+1
      DO 10 N=2,NN
      PHIN=(N-1)*PHID
      COS=DCOS(PHIN)
      T(N)=(BI(N)*BKCP(N)-((DFCP*DFCP)/(DFA*DFA))*BICP(N)*BK(N))*
     2(BID(N)/BI(N))*COS-(1.D0/((N-1)*PI))*((RD/RCP)**(N-1)-(RD*RCP)**(N
     3-1))
      ST=ST+T(N)
   10 CONTINUE
      A0=(BI(1)*BKCP(1)-((DFCP*DFCP)/(DFA*DFA))*BICP(1)*BK(1))*(BID(1)/B
     2I(1))
      A1=(1.D0-RCP*RD)/(1.D0-(RD/RCP))
      Q=A0+2.D0*ST+(2.D0/PI)*DLOG(A1)
      FH=(((-2.D0)*XK**2)*(DFD/DFCP)/(PI*C*EP*K))*Q
      RETURN
      END
```

```
      SUBROUTINE DZH(XK,RC,RCP,KA,A,EP1,EP2,LSP,SSP,R1,R,ZH)
      REAL*8 H1,XK,KA,C,LSP,SSP,H2,EP1,EP,H3,R1,R,D,PI,RC,RCP,EP2,ZH,A
      C=2.998D8
      EP=8.854D-12
      PI=3.14159265358979D3
      H1=XK**2+KA**2*(1.D0-C**2*LSP/SSP)
      H2=XK**2+KA**2*(1.D0-EP1/EP)
      H3=DLOG(R1/R)
      D=(((-2.D0*PI*EP1*EP*H1)-(1.D0/SSP)*H3*H2)*(H3*H1+H3*H2)+(H2*H1
     2*H3)*(2.D0*PI*EP1*EP+(1.D0/SSP)*H3))/(-2.D0*PI*EP1*EP*H1-(1.D0/
     3SSP)*H3*H2)**2-(DLOG((RC-RCP)/R1))/(2.D0*PI*EP2*EP)
      ZH=(2.D0*(XK**2+KA**2)**0.5*A**2/(KA*C))*D
      RETURN
      END
```

```
      SUBROUTINE DGH(XK,PC,RCP,KA,A,NS,NN,GH)
      REAL*8 XRC,XK,RC,XRCP,RCP,DFA,DFC,DFCP,BI(100),BIC(100),BICP(100),
     2BK(100),BKC(100),T1,C1,C2,C3,C4,A,T2,T,ORSUM,PI,BS,CS,SUM,S1,S,KA,
     3EP,GH,C
      PI=3.14159265358979
      EP=8.854D-12
      C=2.998D8
      XRC=XK*RC
      XRCP=XK*RCP
      DFA=DEXP(XK)
      DFC=DEXP(XRC)
      DFCP=DEXP(XRCP)
      CALL BESI(XK,0.D0,NS,BI,100)
      CALL BESI(XRC,0.D0,NS,BIC,100)
      CALL BESI(XRCP,0.D0,NS,BICP,100)
      CALL BESK(XK,0.D0,NS,BK,100)
      CALL BESK(XRC,0.D0,NS,BKC,100)
      T1=0.D0
      DO 5 N=2,NS
      C1=(BICP(N-1)+BICP(N+1))*BIC(N)*RCP+(BIC(N-1)+BIC(N+1))*BICP(N)*RC
      C2=BKC(N)/(DFC*DFC*BIC(N))-BK(N)/(DFA*DFA*BI(N))
      C3=BICP(N)*BIC(N)*(1.D0/(DFC*DFC*BIC(N)*BIC(N))-1.D0/(DFA*DFA*
     2BI(N)*BI(N)))
      C4=DFCP*DFC*A**(0.5D0*XK*XK*C1*C2-XK*C3)
      T1=T1+C4
    5 CONTINUE
      T2=DFCP*DFC*A*(XK*XK*(BICP(2)*BIC(1)*RCP+BIC(2)*BICP(1)*RC)*
     2(BKC(1)/(DFC*DFC*BIC(1))-BK(1)/(DFA*DFA*BI(1)))-XK*BICP(1)*BIC(1)*
     3(1.D0/(DFC*DFC*BIC(1)*BIC(1))-1.D0/(DFA*DFA*BI(1)*BI(1))))
      T=T2+2.D0*T1
      ORSUM=(2.DC/PI)*(DFCP/DFA)*(BICP(1)/BI(1))*((DFA/DFC)*BI(1)*BKC(1)
     2-(DFC/DFA)*BIC(1)*BK(1))
      CALL BSUM(XK,PC,RCP,NS,BS)
      NP=NS+1
      CALL CSUM(XK,RC,RCP,NP,NN,CS)
      SUM=BS+CS
      S1=SUM+(1.D0/PI)*DLOG((1.D0-PC*RCP)/(1.D0-RCP/RC))
      S=(XK*A/(2.DC*(KA/A)*C*EP))*(ORSUM+2.D0*S1)
      GH=(S+T/(2.DC*PI*(KA/A)*C*EP))*((XK*XK+KA*KA)**0.5/XK)
      RETURN
      END
```

WAVE PROPAGATION ALONG A SHIELDED COAXIAL CABLE WITHIN A CIRCULAR WAVEGUIDE

by

JEN - HWANG LEE

B.S.E.E., National Chiao-Tung University, Taiwan, 1972

AN ABSTRACT OF A MASTER'S THESIS

submitted in partial fulfillment of the

requirements for the degree

MASTER OF SCIENCE

Department of Electrical Engineering

KANSAS STATE UNIVERSITY

Manhattan, Kansas

1976

The wave propagation and excitation problem for a coaxial cable within a circular tunnel is examined in this paper. Through study of an idealized model we may obtain understanding of the complicated propagation phenomena inside a real tunnel structure. The tunnel wall is assumed to be perfectly conducting. Within the tunnel is located a dipole antenna and a shielded coaxial cable which are used as excitation source and wave transmission medium respectively. Two shielded coaxial cable models are introduced, from which the external impedance of the cable can be determined. By matching the boundary conditions on the cable surface, we can evaluate the total current on the cable. This current is expressed in terms of two components, those of the bifilar and the monofilar modes. In order to understand the wave behavior inside the tunnel, we investigate the variation of the cable currents of these two modes with respect to the various parameters. Finally, the transmission-line equations are solved, and the current on the center conductor is found.